Exploring multispecies evolutionary dynamics using model microbial ecosystems

by

Hasan Celiker

B.S. Electrical and Electronics Engineering
Bilkent University, 2009

Submitted to the Department of Electrical Engineering and Computer Science
in Partial Fulfillment of the Requirements for the Degree of

Doctor of Philosophy

at

MASSACHUSETTS INSTITUTE OF TECHNOLOGY

June 2014

Signature redacted

Signature of Author: ____
Department of Electrical Engineering and Computer Science
May 7, 2014

Signature redacted

Certified by: _____
Jeff Gore
Assistant Professor of Physics
Thesis Supervisor

Signature redacted

Accepted by: _____
Leslie A. Kolodziejski
Chair of the Committee on Graduate Students

Exploring multispecies evolutionary dynamics using model microbial ecosystems

by

Hasan Celiker

B.S. Electrical and Electronics Engineering
Bilkent University, 2009

Submitted to the Department of Electrical Engineering and Computer Science
on May 7, 2014 in Partial Fulfillment of the Requirements for the Degree of

Doctor of Philosophy

ABSTRACT

Experiments to date probing adaptive evolution have predominantly focused on studying a single species or a pair of species in isolation. In nature, on the other hand, species evolve within complex communities, interacting and competing with many other species. We developed experimental microbial ecosystems with which we can start to answer some of the fundamental questions regarding evolution in complex ecosystems. We first tested how the evolution of cooperation within a species can be affected by the presence of competitor species in an ecosystem. To achieve this, we used sucrose metabolism of budding yeast, *Saccharomyces cerevisiae,* as a model cooperative system that is subject to social parasitism by cheater strategies. We found that when co-cultured with a bacterial competitor, *Escherichia coli,* the frequency of cooperator phenotypes in yeast populations increases dramatically as compared to isolated yeast populations. These results indicate that a thorough understanding of species interactions is crucial for explaining the maintenance and evolution of cooperation in nature. Next, we wanted to explore the question of whether evolution in a multispecies community is deterministic or random. We let many replicates of a multispecies laboratory bacterial ecosystem evolve in parallel for hundreds of generations. We found that after evolution, relative abundances of individual species varied greatly across the evolved ecosystems and that the final profile of species frequencies within replicates clustered into several distinct types, as opposed to being randomly dispersed across the frequency space or converging fully. These results suggest that community structure evolution has a tendency to follow one of only a few distinct paths.

Thesis supervisor: Jeff Gore
Title: Assistant Professor of Physics

Acknowledgements

There are a lot of people without whom this work would not be possible: first and foremost, I would like to thank my supervisor Jeff Gore, for letting me join his group and for his invaluable support and guidance throughout my studies. I wish to also thank Dr. Timothy Lu and Dr. Jongyoon Han for their service on my thesis committee. I am grateful for my colleagues in Gore lab, especially my officemate Eugene Yurtsev for his friendship. Finally and most importantly, I would like to thank my parents Gulsen and Huseyin Celiker, and my brother Orhan Celiker for their love and support throughout all my life.

Table of Contents

INTRODUCTION

Experiments to date probing adaptive evolution have predominantly focused on studying a single species or a pair of species in isolation. In nature, on the other hand, species evolve within complex communities, interacting and competing with many other species. In this thesis, we aim to develop experimental systems with which we can start to answer some of the fundamental questions regarding evolution in such complex ecosystems. The experimental systems we develop consist of microbes. There are several advantages to using microbes to study evolution (1) Microbial model systems are amenable to easy genetic manipulation (2) Generation times of microbes are much smaller than animal models allowing controlled long-term evolution experiments and (3) Microbes are easy and inexpensive to maintain and propagate.

We use these model systems to answer two fundamental questions: (1) How does cooperative behaviors within a species evolve in a complex ecosystems? i.e. Does the presence of other species have any effect on the evolution and maintenance of cooperation within a focal species? (2) How does a community of species evolve as a whole? If we were to replay evolution in a complex multi-species community many times over, would we get the same outcome or different outcome each time?

To answer the first question we developed a microbial ecosystem consisting of two coexisting species: yeast and bacteria. Yeast cells use sucrose metabolism to cooperate with each other. By adding another species (bacteria) we were able to experimentally test the effect of a competitor species on the cooperative dynamics within the yeast population. We found that presence of bacteria can drive the evolution of cooperation within yeast. For the second question, we designed and developed a multispecies community consisting of six soil bacteria species that could robustly coexist in a relatively simple environment. We created many replicates of this model ecosystem and let these evolve for hundreds of generations. At the end, we looked at the differences across replicates in terms of community

structure (relative abundances of species present in the community). We found that after evolution, community structure across the replicates clustered into several distinct types, rather than being randomly dispersed in the frequency space or converging completely.

PART I

Effect of competitor species on the evolution of cooperation within a species

Competition between species is a major ecological force that can drive evolution. Here we test the effect of this force on the evolution of cooperation within a species. We use sucrose metabolism of budding yeast, *Saccharomyces cerevisiae,* as a model cooperative system that is subject to social parasitism by cheater strategies. We find that when co-cultured with a bacterial competitor, *Escherichia coli,* the frequency of cooperator phenotypes in yeast populations increases dramatically as compared to isolated yeast populations. Bacterial competition stabilizes cooperation within yeast by limiting the yeast population density and also by depleting the public-goods produced by cooperating yeast cells. Both of these changes induced by bacterial competition increase the cooperator frequency because cooperator yeast cells have a small preferential access to the public-goods they produce; this preferential access becomes more important when the public good is scarce. Our results indicate that a thorough understanding of species interactions is crucial for explaining the maintenance and evolution of cooperation in nature.

INTRODUCTION

Cooperation is a widespread phenomenon in nature. However, costly cooperative strategies are vulnerable to exploitation by cheats that do not cooperate but freeload on the benefits produced by the cooperating individuals [1,2]. Therefore, the persistence of cooperation in nature has been a puzzling question for evolutionary biologists and there has been much theoretical and experimental

research trying to elucidate the mechanisms underlying this phenomenon [3–6]. Microbial studies have suggested that cooperation can be maintained in nature by mechanisms such as reciprocity[7,8], spatial or temporal heterogeneity[9–11], and multi-level selection[12]. Recently it has become increasingly clear that in addition to population dynamics, external ecological factors can also play significant roles in affecting the evolution of cooperation[13,14].

One such important ecological factor is interspecies interactions[15]. However, almost all laboratory experiments aimed at understanding cooperation have relied on studying a single species in isolation. In contrast, species in the wild live and evolve within complex communities where they interact with other species[16]. Interspecific competition—that is competition between species—has been shown to play a key role in shaping species distributions[17,18] and evolution of character displacement [19,20]. Nevertheless, little effort has focused on establishing a link between this ecological pressure and the evolution of cooperation within a species[21–24]. As one of the few studies that tried to answer this question, Harrison et al found that interspecific competition with *S. aereus* can select for cheats within *P. aeruginosa* for the production of an iron scavenging siderophore molecule. The authors speculated that this result was probably due to increased competition for iron [22]. In another study, computer simulations of biofilms showed that in spatially structured environments, when competition for essential nutrients is strong, the addition of more species can inhibit cooperation within a focal species because the added species can outcompete the cooperating cells [24]. On the other hand, when nutrients were abundant, their model predicted that the public-good producing cells would be surrounded by other species and insulated from cheater cells of the same species, thus cooperators would be favored. In our paper, we aimed to systematically quantify the effect of interspecific competition on the evolution of cooperation using an experimental microbial system, yeast sucrose metabolism. We found that the presence of a bacterial competitor could dramatically increase the cooperator frequency.

Wild-type yeast cells break down extracellular sucrose cooperatively by paying a metabolic cost (Fig. S1) to synthesize the enzyme invertase[25,26]. Invertase is secreted into the periplasmic space between the plasma membrane and the cell wall where it hydrolyzes sucrose to the sugars glucose and fructose. In a well-mixed environment, most of the sugars produced in this manner diffuse away to be consumed by other cells in the population, making the sugars a shared public good. Under these conditions, an invertase knockout strain can act as a cheater that takes advantage of and invades a cooperating population. However, cooperator cells capture ~1% of the sugar they produce due to a local glucose gradient (Gore *et al*, 2009, Dai *et al*, 2012). This preferential access to the public good provides cooperators an advantage when present at low frequency, since in this case there is little glucose for the cheaters to consume (experiments here are done in media with 4% sucrose and 0.005% glucose). The cooperator and cheater strategies are therefore mutually invasible, leading to steady-state coexistence between the two strategies in well-mixed batch culture[26].

RESULTS

Effect of interspecific competition on the evolution of cooperation within yeast

First, we confirmed that there is coexistence between cooperator and cheater strategies in pure yeast cultures. Starting with an initial cooperator fraction of 10%, we observed little change in cooperator frequency after 10 days of co-culture (Fig. 1). In these experiments, every 48 hours we performed serial dilutions into fresh sucrose media and measured the fraction of cooperator cells within the yeast population using flow cytometry (materials and methods and Fig. S2).

To test whether interspecific competition can influence cooperation within the yeast population, we performed the same experiment, but this time co-cultured the cooperator and cheater yeast along with a bacterial competitor, *E. coli* (DH5α). This strain of *E. coli* cannot utilize sucrose[27] but could grow on arabinose (another carbon source present in the media), on the other hand arabinose could not be

utilized by our yeast strains (Fig. S3). We found that the presence of bacteria led to a large and rapid increase in the cooperator fraction in the yeast population over the 10 days of growth. Whereas the cooperator fraction in the pure yeast cultures was only ~14% at the end of the experiment, in cultures with the bacterial competitor the cooperator fraction increased to ~45% (Fig. 1). We also confirmed that this increase in cooperator frequency is not due to a hidden fitness difference between the two yeast strains uncovered by the presence of bacteria. Addition of excess glucose (0.2%) completely eliminated any increase in cooperation in all of the tested conditions, even though bacteria were still present (Fig. S4). Therefore, the increase in cooperator fraction upon addition of the bacterial competitor is indeed related to sucrose metabolism.

A possible explanation for this increase in cooperator fraction within the yeast population is that bacteria behave as a 'superior' cheater strain by assimilating available free glucose, thus depriving cheater yeast cells of any sugar. In such a scenario, cooperator cells would do better than cheaters since they have at least some preferential access to the produced glucose. To test this, we competed yeast against a mutant strain of *E. coli* (JM1100) that has much reduced glucose and fructose uptake rates (materials and methods) [28]. We found a somewhat smaller albeit still significant increase in the cooperator fraction within the yeast population under the same conditions (Fig. 1). Bacterial competition for the public good may therefore be a contributing factor towards increasing cooperator frequency in the yeast population, but there is another mechanism at work as well. We will show later that the other mechanism by which bacterial competition is selecting for cooperator cells in yeast is by limiting the yeast population density.

Two species growth dynamics

To gain insight into the dynamics of competition between the two species, we monitored the optical absorbance of batch cultures seeded with yeast and bacteria. We found that the overall growth follows reproducible successional stages (Fig. 2A). Bacteria have a higher growth rate than yeast and rapidly increase in biomass until

they stop growing early during culture. In contrast, the yeast population takes relatively longer to establish but is able to continue growth after bacteria have stopped dividing. We reasoned that this succession might be due to acidification caused by fermentation, since *E. coli* growth can be severely limited at acidic conditions[29,30]. Indeed, when we monitored the fluorescence of a pH sensitive dye (fluorescein) in the media, we measured a sharp drop in fluorescence (~pH) coinciding with bacterial growth and saturation (Fig. 2A and Fig. S5). This suggests that the limited bacterial growth may be caused by low pH brought about by sugar fermentation. Compared to bacteria, yeast cells are better able to tolerate the harsh acidic conditions[29] present in the later stages and can therefore continue to grow, albeit on depleted resources. In microbial assemblages, such ecological succession is a commonly observed phenomenon[31–33].

We reasoned that if acidic conditions restrict bacterial growth then it should be possible to delay the onset of this limitation by adding more pH buffer in the media. Consistent with this expectation, we found that the final biomass achieved by bacteria increased with the concentration of the pH buffer (PIPES) in the culture (Fig. 2A). We also saw that this increased bacterial density restricted the yeast growth due to pronounced competition between the two species. Prompted by these observations, we decided to use the buffering capacity as an environmental variable to tune the niche overlap and thus the intensity of competition between yeast and bacteria.

Cooperator yeast cells do better under interspecific competition

If cooperator cells were indeed selected as a result of interspecific competition, we would expect to see a positive correlation between the level of final cooperator fractions within the yeast population and the degree of competition imposed by bacteria. To test this, we performed competition experiments with yeast and bacteria as before and varied the buffering capacity of the media. As expected, increasing the buffering further caused the cooperator fractions to increase within the yeast population, but only when competing against bacteria (Fig. 2B).

We next repeated these experiments by starting out with different initial fractions of cooperators (30%, 50%, 90%) and observed the same trend in all the conditions we examined (Fig. S6). Even starting with an initial fraction of 90% cooperators, at high buffering we saw an increase of ~6% in the frequency of cooperators after 10 days of growth. This result suggests that at equilibrium the cheater cells might even be completely purged from the yeast population under the pressure of interspecific competition. Finally, to probe the generality of our results, we competed cooperator and cheater yeast against bacteria on solid agar with sucrose as the sole carbon source. Consistent with the results in liquid cultures, we observed that the presence of bacteria (JM1100) strongly selected for cooperator cells within yeast (Fig S10).

Although in our experiments the cooperator fractions after ten days are not necessarily the values at equilibrium, the rapid increase of cooperator fraction in the presence of bacteria is a striking effect of interspecific competition on the evolution of cooperation. The fact that the change in cooperator frequency is extremely slow in isolated cultures as compared to the change in our two-species competition experiments suggests that even transient bacterial competition can have a lasting impact on the fraction of cooperator cells within yeast populations. In fact, in some of the low buffering conditions the bacterial species went extinct but the cooperator fraction within the yeast population was nevertheless significantly enhanced as compared to isolated yeast populations (Fig S6). Given the importance of non-equilibrium dynamics in nature[34], we believe that these findings may aid in understanding the of evolution of cooperation in wild populations.

To measure the density of the yeast and bacteria in these experiments, we used flow cytometry at the end of each growth cycle (see materials and methods and Fig. S7). We found that by the end of the last cycle, in cultures without any added buffer, bacteria went extinct, whereas at the highest buffer concentration used (20 mM), yeast was outcompeted by bacteria (Fig. 2C). However, at intermediate levels of buffering, yeast and bacteria could stably coexist. This coexistence is a result of the

temporal heterogeneity mediated by acidification and the fact that bacteria and yeast partition into different niches[35] by utilizing different carbon sources in the media (arabinose and sucrose respectively). At high buffer concentrations, cooperator yeast are favored relative to cheater yeast. However, as the total yeast population density decreases with increased buffering (eventually going to zero), the absolute number of cooperator yeast decreases as well. It is therefore important to distinguish between selection for cooperator cells in a population (fraction of cooperators in the yeast population) versus the absolute number of cooperator cells.

Although in co-cultures bacteria went extinct without buffering, in pure cultures we found that bacteria could grow robustly under the same conditions. This observation suggests that the presence of yeast has a negative effect on bacteria. We speculate that faster acidification due to increased glucose concentrations with higher yeast population density combined with ethanol production during the later stages of yeast growth (after bacterial growth stops, i.e. second phase of succession) might be causing bacterial death [29,36]. When we analyzed the overall relationship between yeast density versus bacterial density across all buffer conditions for each cycle and different initial cooperator fractions, we found a consistent negative linear dependence (Fig. 2D). This relationship is the hallmark of interspecific competition whereby the two species reciprocally repress each other's growth[37].

Two-phase logistic yeast growth model

It has been shown that due to the cooperative nature of growth on sucrose, the per-capita growth rate is lower at low cell density and becomes higher as the cell density increases because more of the sucrose has been converted to glucose [26]. Moreover, in these low-density conditions, cooperator cells grow faster than cheaters, as they have preferential access to the produced glucose and 'feel' a higher glucose concentration than cheaters do (Fig. S8). At high cell density, we found that cheaters have a growth advantage over cooperators, since enough glucose can accumulate in the media to support cheater growth.

Using these results, we developed a simple two-phase logistic growth model describing the cooperative dynamics within a pure yeast population in batch culture (see Fig. S8). The model incorporates the fact that in the beginning of a culture, the yeast density is low and there is little glucose in the media because there are not enough cooperators to supply it. Therefore, at the beginning of each growth cycle the cooperators have an advantage. However, as the yeast population grows eventually the density of cooperators increases above a critical value, at which point cheating starts to be favored because now there is enough glucose in the media that cooperators are at a disadvantage by carrying the burden of public good [26]. In the end, the culture logistically saturates to a set carrying capacity, K. This phenomenological model has been previously used to yield accurate quantitative agreement to experimental data for yeast growth in sucrose, including the presence of a fold bifurcation that leads to catastrophic collapse of the population in deteriorating environments (Dai et al, 2012). Moreover, this simple model is quantitatively identical to a more mechanistic model that incorporates changes in glucose concentration over the course of each growth cycle (Fig S11).

Prompted by our experiments with two-species competition, we reasoned that the first order effect of bacterial competition might be to decrease the carrying capacity of the yeast population by depleting essential nutrients in the media (Fig 2D). Indeed, our model predicts that the cooperator frequency should increase as the carrying capacity decreases (Fig 3 and Fig S8 and Fig S11). This increase in cooperation results from the fact that a decrease in the carrying capacity makes the yeast populations spend more time in the low cell density regime (where cooperators have an advantage) and less time in the high cell density regime (where cheater cells have an advantage). Thus, smaller yeast population density mediated by low nutrient availability should increase the frequency of cooperator phenotypes within yeast.

Nutrient limitation causes cooperator frequency to increase within a pure yeast population

If bacterial competition is selecting for cooperator cells within the yeast population via reduced yeast population density, then it should be possible to experimentally induce the same effect even in the absence of bacteria. To test this prediction of our model we limited essential nutrients in pure yeast cultures experimentally. We competed cooperator and cheater yeast cells in uracil limited cultures. Our yeast strains are uracil auxotrophs and require uracil to be supplied in the media to grow (see Materials and methods). As before, we performed serial dilutions every 48 hrs into fresh media and measured the final fraction of cooperators and total yeast density. Consistent with the predictions of our model, we found that the frequency of cooperators increased with decreasing concentrations of supplemented uracil (Fig. 4A). To make sure that this result is not due to an anomaly related to the synthetic nature of auxotrophy, we also repeated this experiment by limiting a universal essential nutrient, phosphate. Again, consistent with our predictions, we observed that the cooperator fraction increased at low phosphate concentrations (Fig. 4B). In all these conditions, we saw that yeast density decreased with limiting concentrations of nutrients as expected. Once again, we observed a negligible change in cooperator fraction in cultures with abundant glucose (0.2%), confirming that the observed behavior is intimately related to the sucrose metabolism.

These results show that limiting the carrying capacity can increase the cooperator frequency within the yeast population. If it is indeed the limited carrying capacity that is causing this effect, then we would expect that the increase in cooperator fractions to be strictly dependent on the yeast density rather than the specific type of nutrient limitation. Consistent with this expectation, when we plotted the final cooperator fraction as a function of the final yeast density for both uracil and phosphate limitation conditions, we found that the resulting relationship was nearly indistinguishable for the two treatments. This observation argues that the underlying force selecting for cooperators was the limited carrying capacity in both cases. Interestingly, we also found that, for both treatments, the final cooperator fraction was approximately linear as a function of the logarithm of the final yeast density (Fig. 4C). Our model could explain this feature of the

experimental data and followed a similar log-linear relationship. All the relevant parameters in the model were consistent with independent experimental measurements (Fig. S8).

Bacteria both limit yeast carrying capacity and act as cheaters

Next, we analyzed our two species competition experiments to see if there is a similar relationship between yeast density and cooperator frequency. We found that competition with bacteria also resulted in a log-linear dependence between yeast density and final cooperator fraction (Fig. 4C and Fig. S9). However, controlling for yeast population density, we found that competition with bacteria was more effective in increasing cooperator fractions within yeast than resource limitation alone. A possible explanation for this difference is that bacteria behave as a 'superior' cheater strain by assimilating available free glucose as we have indicated earlier.

To test this hypothesis, we again competed yeast against our mutant strain of *E. coli* (JM1100) that has much reduced glucose and fructose uptake rates[28] compared to DH5α. In this case, across the same yeast densities, the effectiveness of the bacteria in selecting for cooperators within yeast decreased significantly, although the final increase in cooperator fractions was still higher than the resource limitation treatment. This result suggests that competition for glucose and fructose is the reason why bacterial competition favors cooperator cells more than resource limitation alone (controlling for yeast population density).

To account for glucose consumption by bacteria in our phenomenological model we made the cheater growth rate at low cell density a linearly decreasing function of the final bacterial density (which is linearly related to the yeast carrying capacity, Fig 2D). We found that this simple assumption could reliably reproduce the effect of bacterial competition on the evolutionary dynamics within the yeast population (fig 4C). By fixing the final yeast density in our model (yeast carrying capacity not limited by bacteria), we found that bacterial competition for glucose alone

significantly underestimated the final cooperator fraction. Taken together, these results indicate that bacterial competition for both essential resources and glucose increases the frequency of cooperators within the yeast population.

We note that this selection of cooperator cells by bacteria is occurring in a yeast growth regime where there is little to no transfer of benefits between yeast cells (i.e. low cell density conditions). Therefore, the cooperator cells are favored by bacteria not because they "cooperate" with other cells, but because they have private access to some of the glucose that they create. The cheater cells are therefore deprived of glucose due to the presence of bacteria (either by direct glucose consumption or by limiting yeast density, which limits the amount of sucrose broken down). So, bacterial competition actually selects for "invertase producing cells" rather than "cooperators" per se. However, since the invertase producing cells are breaking down sucrose outside of the cell, ~99% of the resulting glucose diffuses away before it can be captured (Gore *et al*, 2009). All cells in the population then benefit from this sucrose hydrolysis during the high-density growth phase, where the bulk of yeast growth occurs in our experiments (see Fig 3 and Fig S8). Selection for invertase producing cells during the first phase of growth (when yeast density is low) then indirectly acts as a stabilizing agent for the cooperator genotype in the yeast population.

A glucose producing bacterial species can select for cheats within the yeast population

Finally, we asked how the cooperative dynamics within yeast would be affected if the competing bacteria were also producing glucose just like cooperator yeast. We found previously that bacterial competition for the public good could select for cooperators within the yeast population beyond that expected based on resource competition alone. If the competing bacteria instead produce the public-good then it may even be possible for the bacteria to favor cheating behavior within the yeast population. To test this, we inoculated yeast cells on sucrose plates together with the soil bacteria *Bacillus subtilis* instead of *E. coli*. Similar to wild-type yeast, *B.*

subtilis breaks down sucrose with a secreted enzyme and generates extracellular glucose[27]. Interestingly, we found that now cheating is favored within the yeast population (Fig S10). Control competition experiments on glucose only media resulted in no difference among various treatments, strongly suggesting that glucose production by *B. subtilis* is responsible for the decrease in cooperator phenotypes on sucrose plates. Thus, it seems that although *B. subtilis* cells compete for resources with yeast, they can produce enough glucose to reverse selection for cooperators within the yeast population. We therefore conclude that other competing species do not necessarily select for cooperators within a species. Thus, caution must be taken in assessing the effect of one species on the other, as the nature of the interaction can drastically modulate the outcome.

DISCUSSION

Our results indicate that social evolution within a species can be greatly affected by interspecies interactions. Specifically, we found that interspecific competition for essential nutrients can limit the carrying capacity of our focal species, yeast, and therefore increase the frequency of cooperator phenotypes. In nature, such interspecific competition is ubiquitous and one of the major factors limiting species ranges [38]. This fact suggests that our findings should be relevant where communities of species coexist and occupy partially overlapping niches. Evolution of cooperation is strongly related to population density. In general, cooperators feel the burden of exploitation by cheater phenotypes at high population densities[6,39]. Our results show that interspecific competition can limit the overall population density of the focal species, and therefore drastically alter the outcome of competition between cooperators and cheaters. As discussed before, this result is due to the fact that cooperators have an advantage in low-density conditions, since they have preferential access to the produced public-goods.

Next, we also showed that competition between species directly for the public-goods produced by one of them can select for cooperators within the producing species. In our experiments, bacteria deplete the public good available for both

cooperator and cheater yeast, but since cooperators have a "private" access to some of the glucose produced they grow faster than cheaters during the initial period of low cell density. Such competition between species for a public-good is a common phenomenon in nature. Among microbial organisms, there are many cases whereby the diffused products of extracellular enzymes can be assimilated by other species of microbes—examples include the extracellular products of siderophore metabolism[22,40], cellulose degradation[41,42], starch[43] and inulin[44] degradation. Therefore, maintenance of the production of these public-goods by one species might be mediated by the presence of other species occupying the niche space where cheaters within the same species would have to radiate into. It is often the case that public-good producing individuals benefit preferentially from being producers, mainly because of spatial heterogeneity (viscous environments in which the produced extracellular products form a diffusion gradient around the producing individuals). This is analogous to our experimental system where we have spatial heterogeneity (despite the fact that we use a well-mixed environment) simply because of the biophysical features of the yeast cell wall. We speculate that such maintenance of cooperation through interspecific competition for public goods might also be present within animal populations, such as primary cavity excavation by woodpeckers (abandoned nests can be utilized by non-excavating bird species instead of next generation woodpeckers, forcing woodpeckers to excavate new cavities)[45], cooperative hunting by hyenas (exploitative competition from lions and mammalian carnivores for the captured prey)[46] etc.

In conclusion, our findings provide evidence for an important ecological mechanism—competition between species—for the evolution of public-goods cooperation within a species. Our results also suggest that cooperation may be more stable than would be concluded from experiments that study a single species in isolation. These findings can help explain the apparent ubiquity of cooperative traits found in nature and improve our understanding of social evolution in natural microbial communities[23]. Our findings also indicate that depending on the nature of interspecific interaction (e.g. competition vs mutualism), other species may also

disfavor cooperation within a species as we have seen in our experiments with *B. subtilis*. Our two species community, which consists of widely used model organisms, is amenable to genetic manipulation and can be reconfigured to explore more complicated interactions between species—such as parasitism and warfare—that may affect within-species cooperation.

MATERIALS AND METHODS

Strains

All yeast (*S. cerevisiae*) strains were derived from haploid cells BY4741 (mating type **a**, EUROSCARF). The 'wild-type' cooperator strain has an intact *SUC2* gene and yellow fluorescent protein (yEYFP, gift from G. Stephanopoulos) expressed constitutively by the *TEF1* promoter inserted into the *HIS3* locus using the backbone plasmid pRS303. The mutant cheater strain lacks the *SUC2* gene (EUROSCARF, *suc2Δ::kanMX4*) and has the red fluorescent protein tdTomato expressed constitutively by the *PGK1* promoter inserted into the *HIS3* locus using the backbone plasmid pRS303. Both of these strains had the same set of auxotrophic markers: *leu2Δ0, met15Δ0, ura3Δ0*. Both *E.coli* strains were derived from *E.coli* K-12. JM1100 was obtained from The Coli Genetic Stock Center (CGSC#: 5843). JM1100 strain (*ptsG23, fruA10, manXYZ-18, mgl-50, thyA111*) could grow on minimal media without additional thymine probably due to a picked up *deoC* mutation, therefore no additional thymine was used in the media for experiments with this strain. *Bacillus subtilis* 168 was obtained from ATCC (#23857).

Batch culture media

All experiments were performed in defined media supplemented with the following carbon sources: 4% sucrose, 0.2% l-Arabinose and 0.005% glucose. For experiments with excess glucose, extra 0.2% glucose was added to cultures. Our default defined media consisted of 0.17% yeast nitrogen base (Sunrise Science) plus ammonium sulfate (5 g/L) supplemented with the following amino acid and nucleotide mixture: adenine (10 mg/L), l-arginine (50 mg/L), l-aspartic acid (80 mg/L), l-histidine (20

mg/L), l-isoleucine (50 mg/L), l-leucine (200 mg/L), l-lysine (50 mg/L), l-methionine (20 mg/L), l-phenylalanine (50 mg/L), l-threonine (100 mg/L), l-tryptophan (50 mg/L), l-tyrosine (50 mg/L), l-uracil (20 mg/L), l-valine (140 mg/L). For uracil limitation, uracil concentration was varied below the amount used in the default media. Uracil concentrations used in Fig 3C: 1, 2, 4, 6, 10, 14 mg/L. Phosphate limited media contained 0.071% yeast nitrogen base without KH_2PO_4 (Sunrise Science) supplemented with 80 mM K_2SO_4 and the amino acid mixture used in the default media. To limit phosphate concentration, KH_2PO_4 was added to this media below the concentration (7.3 mM) used in the default nitrogen base. KH_2PO_4 concentrations used in Fig 3C: 0.01, 0.03, 0.05, 0.1, 0.2, 0.3 mM. In all the experiments, pH was adjusted to 6.5 with NaOH and PIPES (pKa 6.8 @ 25°C) was used as a buffering agent for different conditions. For nutrient limitation experiments, a set PIPES concentration of 10 mM was used for all the conditions. In competition experiments with DH5α, a buffer range of 0-20 mM was used. We found that JM1100 was more acid tolerant than DH5α, therefore a narrower range of 0-10 mM of buffering was used for this strain.

Growth conditions

Before each experiment, yeast strains were grown in minimal media (2% glucose) for 20h at 30°C and bacterial strains were grown in LB at 37°C for 20h. These initial cultures were diluted in fresh media to start the experiments. In all the experiments described, initial inoculation densities were 10^6 cells/mL for bacteria and $7.5x10^4$ cells/mL for yeast. These initial inoculation densities were chosen based on preliminary experiments where average densities of two species after stable coexistence was measured. This ensured that bacteria and yeast would not outcompete each other initially by simple overabundance of one species versus the other. All experiments were performed in 96-well microplates containing 150 μL media per well. To enable gas exchange, microplates were sealed with two layers of a gas permeable tape (AeraSeal) and incubated at 30°C, 70% relative humidity, shaken at 825 r.p.m. Evaporation per well was measured to be 20% over 48h. For

multi-day experiments, cultures were serially diluted 1:1,000 into fresh media every 48 hrs, taking evaporation into account.

Flow cytometry

Grown cultures were diluted 1:100 in PBS (phosphate buffered saline) and cells were counted on BD LSR II equipped with an HTS unit. For each well, two separate measurements using different settings were taken for yeast and bacteria. For measuring cooperator fraction and yeast density, a high SSC threshold (300) with SSC voltage 200 V was used to exclude bacterial counts (FSC voltage, 270 V). Cooperator and cheater yeast strains were gated on fluorescence (YFP and RFP respectively). For each well, 20 μL of sample was measured with flow rate 1.5 μL/sec. Yeast was assumed to be extinct in wells with less than 400 counts and cooperator fraction was not calculated for these cases. To estimate the yeast population density, a calibration was used with measurements of yeast cultures with known densities. To measure bacterial density, SSC voltage was set to be 300 V with threshold 1000 to capture all the bacterial population. For each well, 5μL sample was analyzed with flow rate 0.5 μL/sec. Bacterial counts overlapped with noise in FSC and SSC plots. To distinguish bacteria from noise, in every cycle, pure yeast culture controls was measured with the same settings used for bacteria (Fig. S8). From these control measurements, noise was calculated and found to have a maximum coefficient of variation less than 0.03. To calculate actual bacterial counts, mean noise of 8 control wells of pure yeast cultures was subtracted from bacterial counts in each competition experiment. In conditions where bacterial population was not extinct, the bacterial counts with noise subtracted were always larger than the noise counts; therefore the variation in noise had little effect on bacterial density measurements. Bacterial density was estimated based on a calibration obtained by measurements of bacterial cultures with known densities.

Successional growth assay

Yeast and bacteria were grown and diluted in fresh media with initial densities same as described in 'growth conditions' section. Initial cooperator fraction was

50%. Culture media was the default media used in all two species competition experiments and cells were grown in microplates. Cultures were incubated using an automated shaker Varioskan Flash (Thermo Scientific) at 30°C, 800 r.p.m. To monitor pH, 0.6 μM fluorescein sodium salt (Sigma) was added to cultures. Every 15 minutes, absorbance (600 nm) and fluorescence (excitation: 488 nm, emission: 521 nm) measurements were taken for 40h.

Competition on agar plates

Solid agar media was prepared using 1.6% agar, 1% yeast extract, 2% peptone supplemented with either 2% glucose or 2% sucrose. Cells were spread on plates (100 mm diameter) containing 20 mL solid media using glass beads. In all the conditions, initial cooperator yeast to cheater yeast ratio was 1:5 (~17% cooperators). Plating density for yeast was aimed to be ~900 cells/plate (15 cells/cm^2), for JM1100 it was ~12 cells/plate (0.2 cells/cm^2) and again for *B. subtilis* ~12 cells/plate (0.2 cells/cm^2). Inoculated cultures were incubated for 4 days at 30°C until no further growth could be observed. Then, plates were illuminated under a blue light (~470 nm) transilluminator (Invitrogen) and imaged through an orange filter. Later, plates were destructively sampled by washing off colonies in PBS. Fractions were measured on BD LSR II flow cytometer using the yeast settings (see flow cytometry section). We used JM1100 instead of DH5α in these experiments because DH5α formed minute colonies on 2% Glucose agar due to excessive acidification. We also tried competing yeast against *B. subtilis* in liquid well-mixed culture, however we could not get coexistence of the two species, and *B. subtilis* was outcompeted by yeast, presumably due to the less acid tolerant nature of this bacterium compared to *E. coli*.

Glucose and fructose uptake measurements for *E.coli* strains

DH5α and JM1100 strains were grown overnight at 37°C in LB and then diluted into media containing 0.2% arabinose plus either 0.05% glucose or 0.05% fructose. Initial cell density for each strain was 5x10^6 cells/mL. For DH5α and JM1100, media

contained 8 mM and 4 mM buffer respectively. After inoculation, 5 mL cultures were incubated at 30°C in 50 mL falcon tubes shaking at 300 r.p.m. Sugar uptake rates were determined by measuring the depletion of sugars during exponential growth according to the following equation[47]:

$$r = \mu \frac{S_0 - S(t^*)}{N(t^*) - N_0}$$

where r is the uptake rate of sugar and μ is the growth rate measured during exponential phase. N is the cell density inferred from optical density measurements. S represents the measured sugar concentration in the media. Measurements taken at two time points separated by t^* were used to calculate the uptake rates. The timing of the two measurements was chosen so that there was substantial depletion in sugar concentration during that period. Glucose concentration was determined by using a commercial glucose (hexokinase) assay reagent (Sigma). Fructose concentration was measured by using the same assay reagent in conjunction with the enzyme phosphoglucose isomerase (PGI), which converts fructose 6-phosphate to glucose 6-phosphate. Glucose uptake rates for DH5α and JM1100 were found to be 4.14×10^4 molecules s^{-1} $cell^{-1}$ and 0.72×10^4 molecules s^{-1} $cell^{-1}$ respectively. Fructose uptake rates for DH5α and JM1100 were found to be 0.47×10^4 molecules s^{-1} $cell^{-1}$ and 0.08×10^4 molecules s^{-1} $cell^{-1}$ respectively.

FIGURES

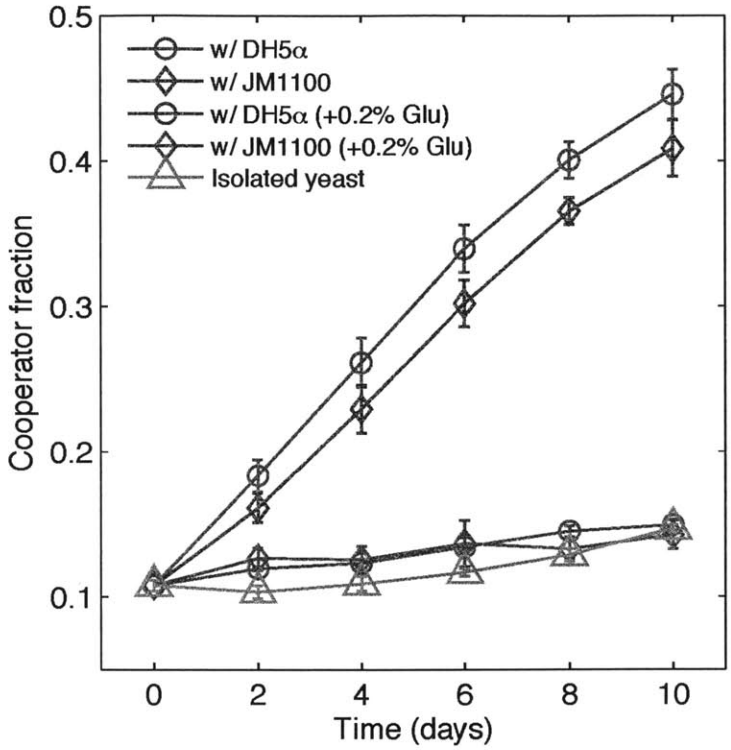

Figure 1: When co-cultured with bacteria in sucrose media, cooperator cell fraction increases within yeast populations. Both with E. coli strains DH5α or JM1100 – a mutant strain that grows poorly on glucose and fructose – a significant increase in cooperator fraction was observed compared to a pure yeast culture (isolated yeast) over 10 days of growth. Addition of excess glucose (+0.2%) to these cultures eliminated this increase in cooperator fraction, indicating that selection for cooperators is linked to sucrose metabolism. In this experiment, culture media contained 4 mM buffer (PIPES). Total final yeast and bacterial densities did not change significantly over the course of five cycles of growth (Fig S9). Error bars, ± s.e.m. (n = 3).

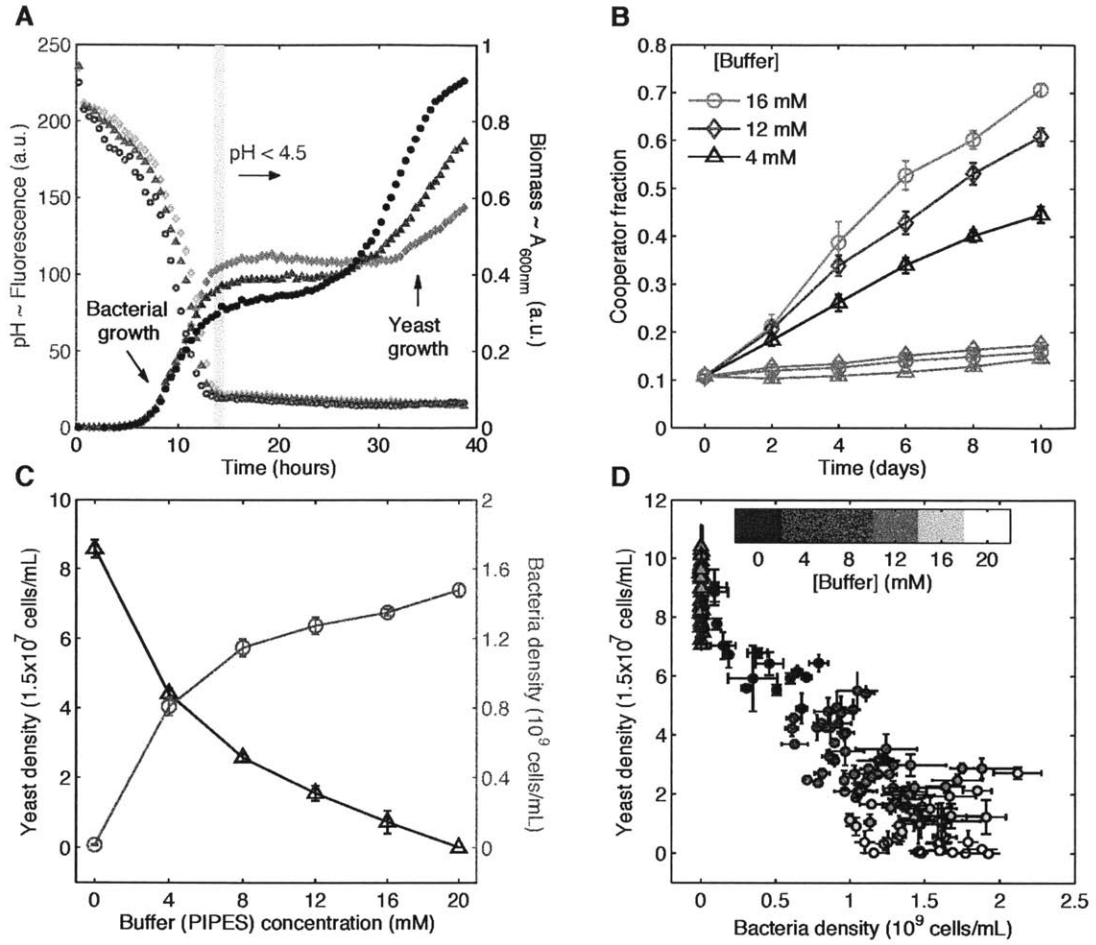

Figure 2: Correlation between the intensity of interspecific competition and cooperator cell frequency within yeast. (A) Successional growth dynamics in mixed cultures of yeast and bacteria. Absorbance (600 nm) was measured for different buffer (PIPES) concentrations: 4 mM (circles), 8 mM (triangles), 12 mM (diamonds). Simultaneously, fluorescence of a pH sensitive dye (fluorescein) was measured and a sharp pH drop was observed coinciding with bacterial growth. Note that as the buffering increases, the pH drop is slower and the final bacterial biomass is higher. Initial pH was 6.5 (~220 fluorescence a.u.) in all the cultures used in our experiments (see methods and Figure S5B). **(B)** Frequency of cooperators within yeast increases faster with increasing buffer concentration when competing against bacteria. Isolated control populations under the same conditions displayed little change in cooperator fraction (orange symbols). **(C)** Yeast (triangles) and bacterial

(circles) density at the end of the last growth cycle as a function of buffering capacity. **(D)** Yeast density versus bacterial density across all buffer concentrations and different initial cooperator fractions for each cycle (initial fractions: 0.1, 0.3, 0.5, 0.9). Control cultures (isolated yeast) for the same conditions are shown in triangles. Error bars, ± s.e.m. (n = 3).

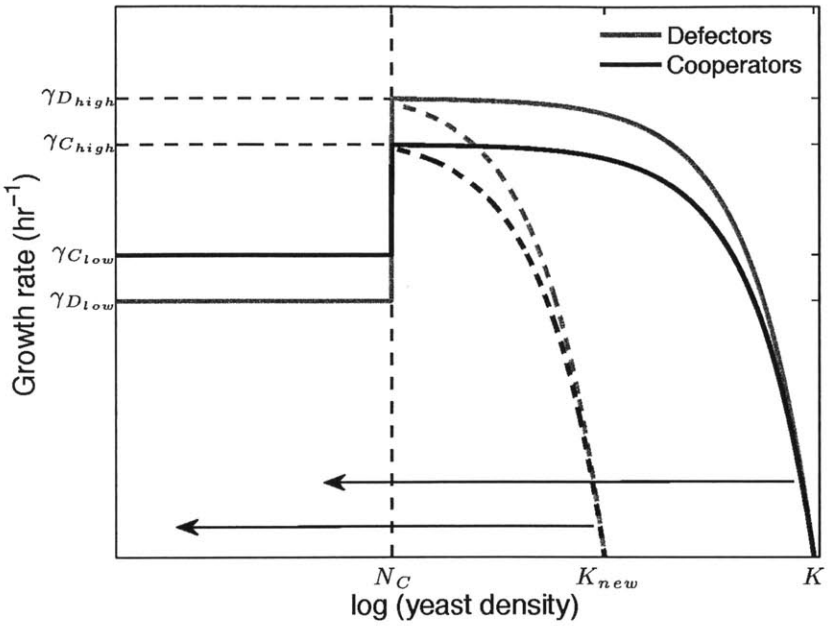

Figure 3: A phenomenological model describes the growth dynamics of cooperator and cheater yeast during each cycle of batch culture This sketch of our yeast growth model describes how the per capita growth rate changes as a function of yeast density. At low density, cooperators have a higher growth rate than defectors. Above a yeast density N_C where cooperator density is at a critical value, it is assumed that the growth rate is higher for both cooperators and cheaters since glucose has accumulated in the media[26]. Then, the growth rate decreases logistically to zero as the yeast density reaches its carrying capacity, K. If the yeast carrying capacity were limited (K_{new}), starting yeast density would be lower after dilution into fresh media.

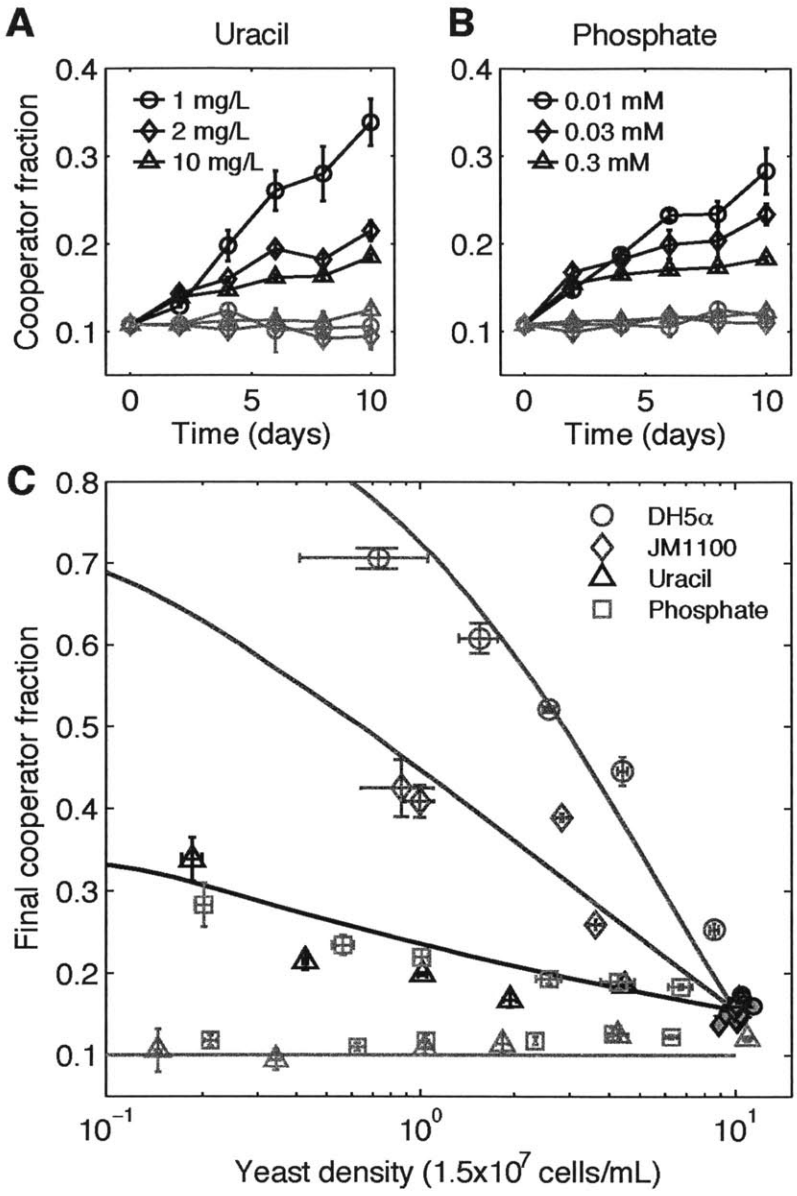

Figure 4: Nutrient limitation can select for cooperator cells within the yeast population even in the absence of bacteria. Limiting either uracil (**A**) or phosphate (**B**) increases frequency of cooperators within isolated yeast populations. Control cultures (gray symbols) with excess glucose (0.2%) displayed negligible change in cooperator frequency. **(C)** Final cooperator fraction versus final yeast density in bacterial competition and nutrient limitation experiments: DH5α, JM1100, uracil, phosphate. Note that for both of the limiting nutrients (uracil and

phosphate) yeast density vs cooperator fraction relationships are extremely similar, indicating that the underlying force for increase in cooperator fraction is the limited carrying capacity. With controls: uracil + 0.2% Glucose (gray triangles), phosphate + 0.2% Glucose (gray squares). Controls (isolated yeast) for competition with bacteria are shown in orange circles and diamonds for DH5α and JM1100 conditions respectively. Solid lines are model simulations for each condition. Error bars, ± s.e.m. (n = 3).

SUPPLEMENTARY FIGURES

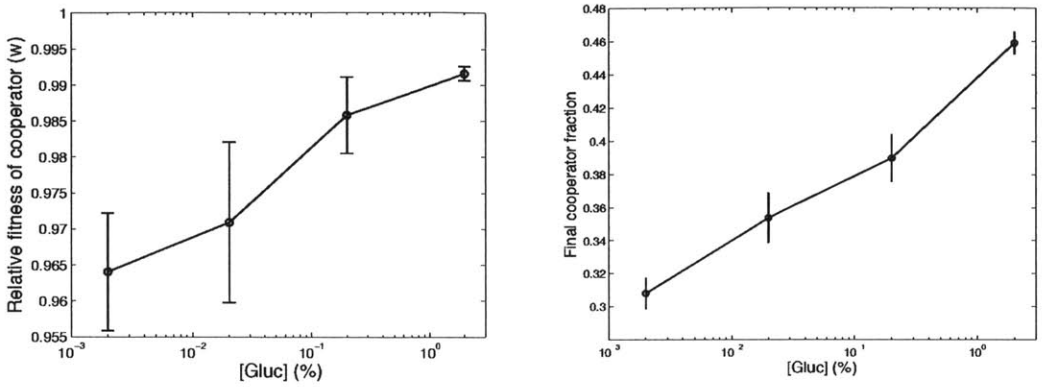

Figure S1: Metabolic cost of invertase production. Invertase expression is maximal at low glucose concentrations but repressed when glucose is abundant[48,49]. We measured the metabolic cost of invertase production by co-culturing cooperator and mutant cheater yeast strains in media containing only glucose as carbon source, by daily serial dilution (1:1,000) for three days. Starting cooperator fraction was 50% and initial cell density was 1.5×10^5 cells/mL. At high concentrations of glucose, invertase expression is repressed and as expected, there was little fitness difference between the two strains. On the other hand, at low concentrations of glucose where invertase expression reached to its maximum, the cooperator strain had a fitness deficit of ~3-4% consistent with a metabolic cost associated with production and secretion of invertase. Left panel shows the relative fitness (w) values which are calculated using the following expression[25]:

$$w = \ln\left[\frac{D_f f_f}{D_i f_i}\right] \Big/ \ln\left[\frac{D_f(1-f_f)}{D_i(1-f_i)}\right]$$

where f_i and f_f are the initial and final cooperator fraction and D_f and D_i are the final and initial total cell densities for each day. Right panel shows the final fraction of cooperators in the same experiment after three days of transfers. Data points represent mean of 3 measurements over 3 days with error bars ± s.e.m.

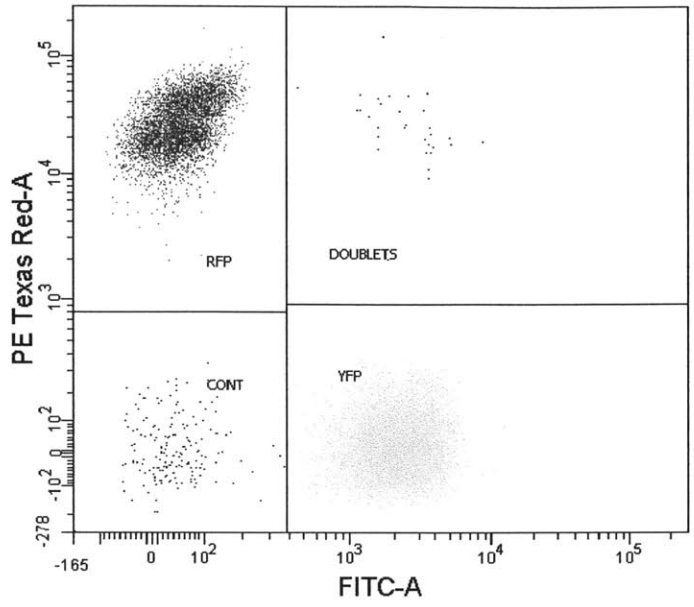

Figure S2: Measurement of cooperator fraction with flow cytometry. Our yeast strains were tagged with constitutively expressed YFP and RFP proteins (cooperator and cheater respectively). We could distinguish between the two strains on BD LSR II flow cytometer. YFP was excited with a blue laser (488 nm) and emission was collected through a 530/30 nm filter (FITC-A channel). RFP was excited with a yellow/green laser (561 nm) and emission was collected through a 610/20 nm filter (PE Texas Red-A channel). The dot plot in the figure is a sample from a competition experiment between yeast and bacteria after 10 days of co-culture. The two strains were well separated on the different fluorescence channels. Cooperator fraction and final yeast density in each well were measured using yeast settings on the flow cytometer (see Methods).

A

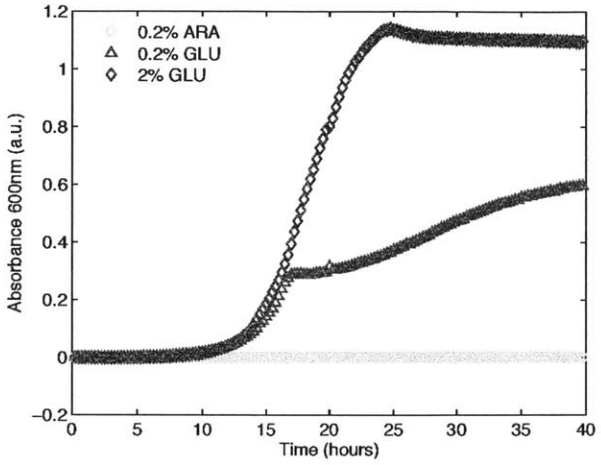

B

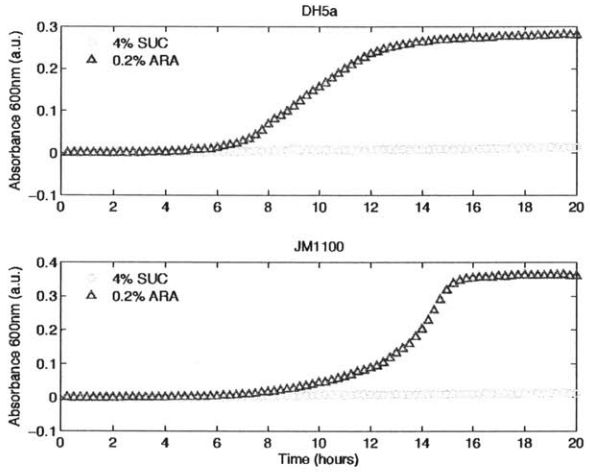

Figure S3: Yeast growth on arabinose and *E.coli* growth on sucrose. (A) We grew yeast (50% cooperator) on 0.2% arabinose, 0.2% glucose or 2% glucose. Initial cell density was the same as in the competition experiments (7.5×10^4 cells/mL). Absorbance at 600 nm was measured for 40 hrs. The results are plotted in the above figure. Our yeast strains were not able to grow on 0.2% arabinose. (B) *E.coli* strains were grown on either 4% sucrose or 0.2% arabinose. Our *E.coli* strains were not able to grow on sucrose.

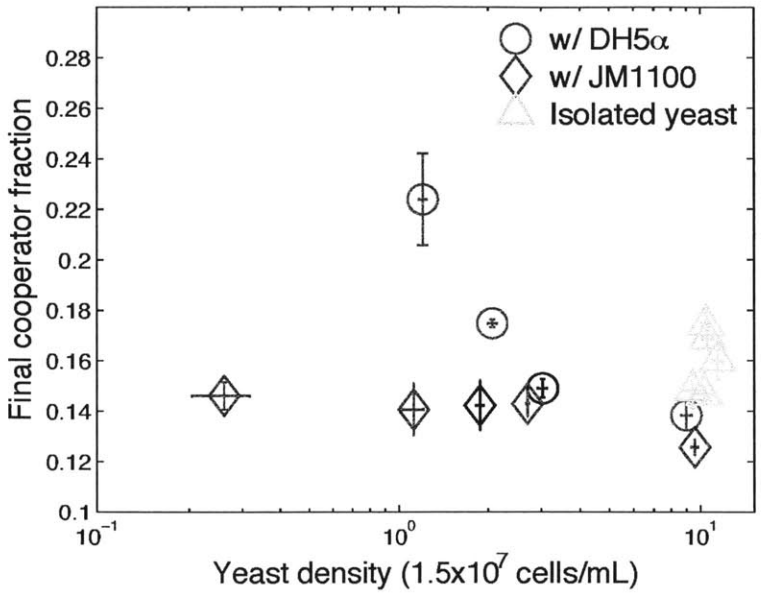

Figure S4: Excess glucose eliminates selection for cooperators in the presence of bacteria. Cooperator fraction after 5 cycles of dilution (10 days of growth) and corresponding final yeast density in competition against bacteria on default media (see Methods). Starting cooperator fraction was 10% for all the data presented. For the conditions with a bacterial competitor (w/ DH5α and w/ JM1100) media contained additional 0.2% glucose. Each individual data point represents the result for a different buffer concentration used. We see that although the yeast density is limited by the presence of bacteria, there is little increase in cooperator fractions when there is excess glucose in the media. Isolated yeast data (triangles) show the highest density yeast population can reach without the presence of bacteria. Black data points are the results for the condition used in figure 1 (4 mM buffering). The reason that the number of data points differ between DH5α and JM1100 treatments is that with DH5α yeast went extinct at some of the highest buffer conditions used and fractions were not calculated for those cases (see Methods).

In addition to these controls, we also tried to grow yeast on media spent by bacteria. To achieve this, we first grew bacteria on default media with varying buffer

concentrations. Then, bacteria were spun down and yeast was grown in the supernatant with added glucose (0.2%) for 48 hrs. The results showed no change in the cooperator fraction, again ruling out a fitness difference between our two yeast strains that might be mediated by bacterial resource depletion. However, we could not dilute and propagate these cultures into new spent media, as the final yeast density was much lower than we observed in our competition experiments. Error bars, ± s.e.m. (n = 3).

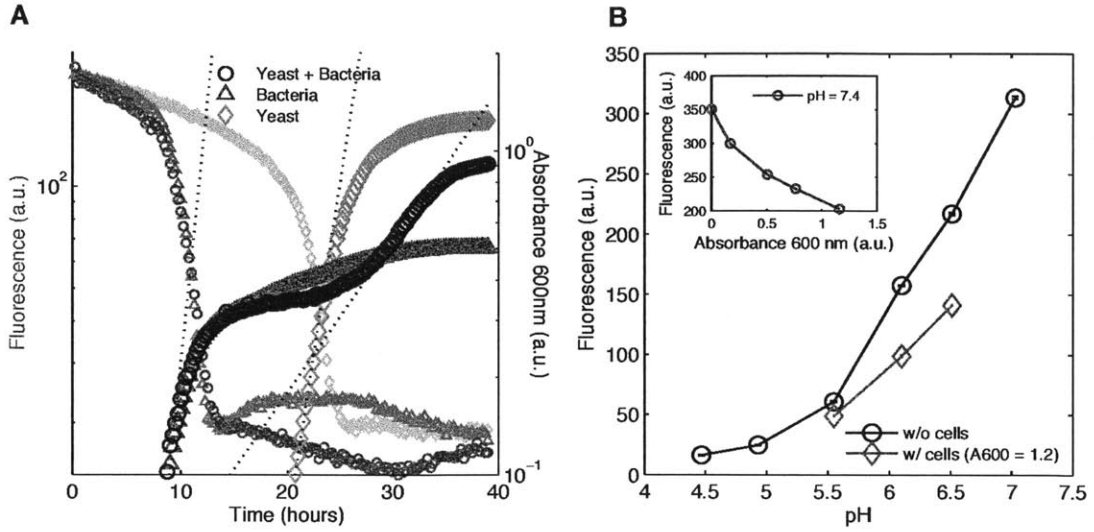

Figure S5. Successional growth dynamics in mixed batch culture. **(A)** Absorbance and fluorescence (~pH, see Methods) measurements for a co-culture of bacteria (DH5α) and yeast, an isolated bacterial culture and an isolated yeast culture. Initial cell densities were as described in Methods and were the same for each species in competition with the other species or by itself. All cultures were buffered with 4 mM PIPES. Dotted lines are the tangents to the absorbance traces during exponential growth. We see that the initial drop in pH in the mixed culture coincides with the pH drop in the isolated bacterial culture, which indicates that initial acidification in the mixed culture is strongly mediated by bacterial fermentation. In contrast, pH drop occurs much later in the isolated yeast culture, as the yeast population takes longer to establish. **(B)** Fluorescein vs. pH calibration curve with and without cells in the media. pH of our default media was adjusted using NaOH without any added buffer and fluorescence was measured as described in Methods. Fluorescein was fluorescent across the relevant pH range (~4.5 to 6.5) and lost its fluorescence completely around pH 4.5, which is also quite close to the pH value where bacterial growth is limited[30]. The drop in pH shown in (a) and figure 2a is not due to accumulating cell mass obscuring fluorescence measurement. By suspending yeast cells in the media at a density of 15×10^7 cells/mL ($A_{600} \sim 1.2$) – which is the maximum density we observed in our experiments – we show that although there is a drop in fluorescence due to the presence of cells, it is not as dramatic as measured

during growth. Inset shows the fluorescence versus absorbance (~cell density) relationship measured by suspending yeast cells in PBS (pH = 7.4) at different densities. Error bars, ± s.e.m. (n = 3).

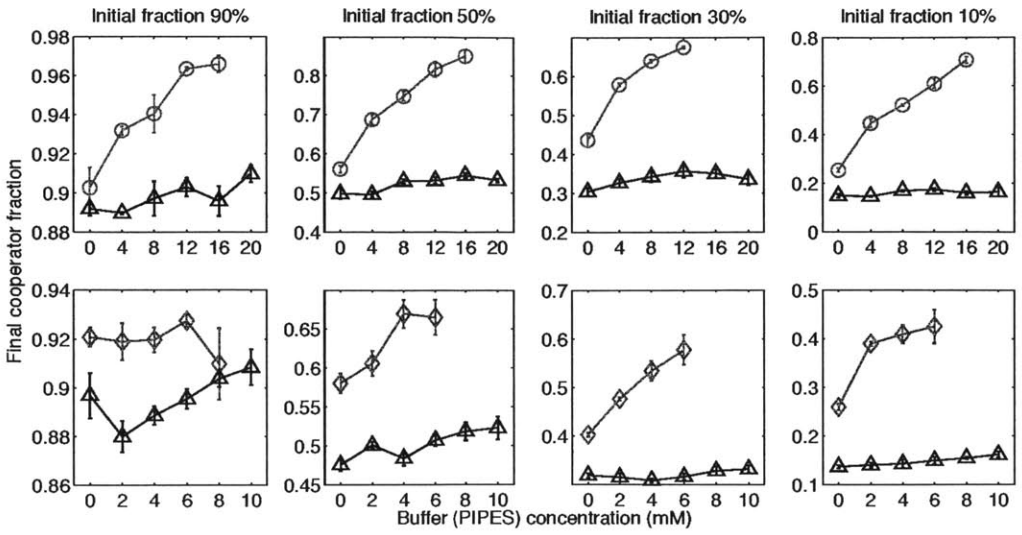

Figure S6: Competition between yeast and bacteria with different initial cooperator fractions. Each individual plot shows the final cooperator fraction (after 10 days of growth) as a function of buffer concentration in the media. Top row shows the results for competition between yeast and DH5α (circles) and the bottom row shows the results for competition between yeast and JM1100 (diamonds). In all the plots, pure yeast controls are shown in triangles. Note that when competing against DH5α, even starting with 90% initial cooperator frequency, cooperator fraction increased in most of the buffering conditions, suggesting that at equilibrium yeast population might consist of only cooperators. For experimental details see Methods. Error bars, ± s.e.m. (n = 3).

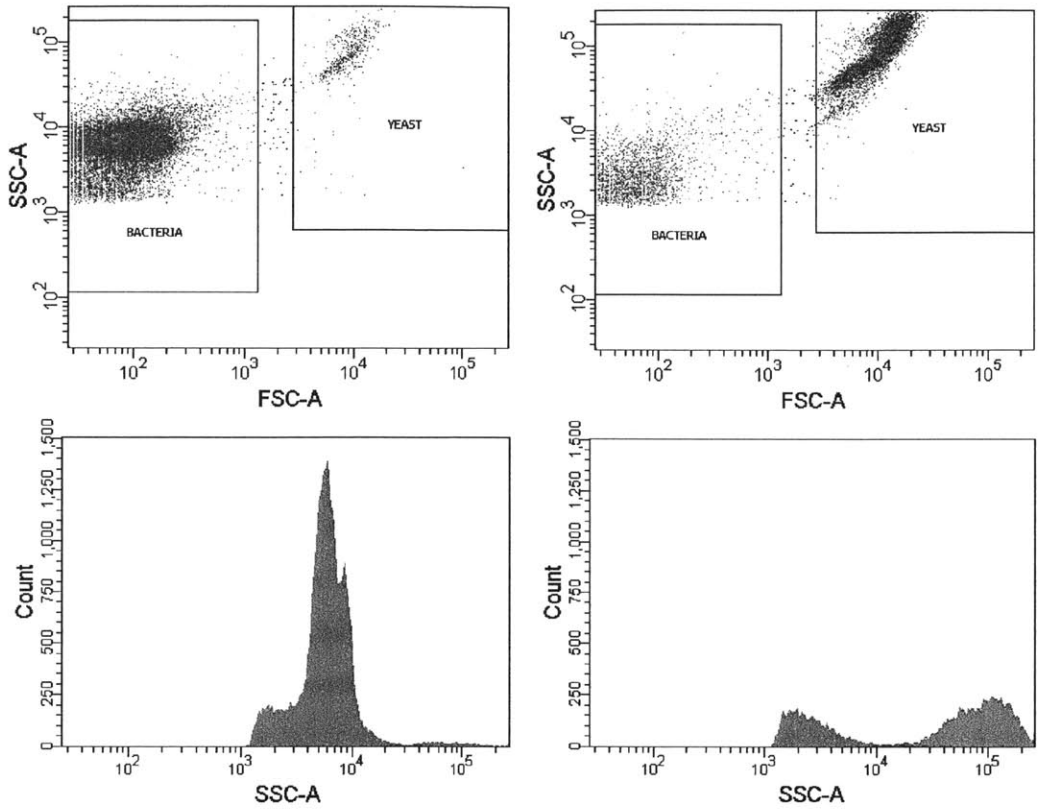

Figure S7: Bacterial density measurements using flow cytometry. Left column shows a typical bacterial density measurement from a two species competition culture. This particular sample is competition after 10 days of growth with 30% initial cooperator fraction and 12 mM buffer (PIPES). To collect the data, bacterial settings were used on the flow cytometer (see Methods). As seen in the top SSC/FSC plot, bacteria (red) and yeast (blue) populations were well separated and easily distinguished. Bottom plot shows the histogram SSC counts for the same condition. In this histogram, skewed left tail of the bacterial counts is due to noise overlapping with the bacterial population counts. To quantify the noise and subtract it from bacterial counts, every growth cycle we measured event counts occurring in the 'BACTERIA' gate for 8 pure yeast cultures (isolated yeast controls) again using the bacterial settings. Right column shows a typical result from such a measurement. This particular sample is from a culture after 10 days of growth with 30% initial cooperator fraction and 12 mM buffer (PIPES) – same as the conditions used in the

left column except without bacteria. Top right plot shows SSC/FSC plot with noise appearing in the region where bacteria was before. In the SSC histogram for this sample (bottom right plot), we see that noise counts overlap nicely with the left tail of bacterial counts from the sample with bacteria (bottom left plot). Bacterial counts in mixed culture experiments were corrected by subtracting the mean of such 8 controls from each sample for every different microplate measurement.

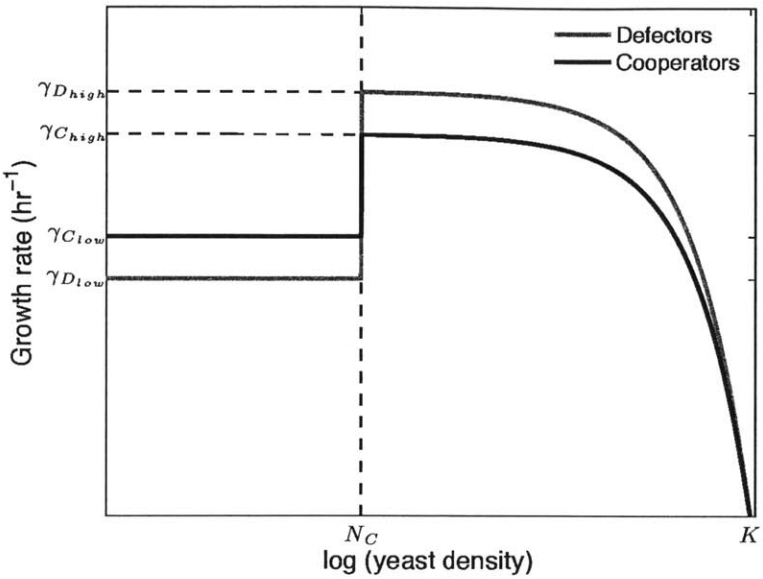

Figure S8: Two-phase logistic growth model. To model the cooperative dynamics within the yeast population, we developed a simple growth model based on experimental measurements. It has been shown that due to the cooperative nature of growth on sucrose, yeast growth rate is lower at low-density conditions and becomes higher as population density increases [26]. We have measured the low-density and high-density growth rates of cooperating yeast populations (as reported below) and confirmed that this was indeed the case. This observation led us to develop a two-phase growth model whereby during the low-density conditions (initial stages of batch culture) yeast growth rate is lower compared to the later stages of the culture where the cell density is higher and faster glucose accumulation occurs. Furthermore, it was shown that when grown separately in low-density conditions, the cooperator growth rate was higher than cheater (defector) growth rate on media containing low glucose concentrations but high concentrations of sucrose [26]. This result was expected, as cheater cells effectively cannot utilize sucrose, while cooperator cells can break down sucrose and capture some of produced products before they get diluted away in the well-mixed environment that was experimentally imposed. This conclusion was further

supported by experiments in which we observed that if the dilution factor between successive cycles of batch growth was higher (>1,000) or cycle length was shortened (24 h instead of 48 h)—thereby imposing low-density conditions—cooperator frequency increased faster in mixed cultures of cooperator and cheater yeast cells. Therefore, we chose to assign a lower value to cheater growth rate at low-density conditions (described in detail below). Since our experiments are performed in batch culture, to simulate the nutrient limited nature of the total growth and final biomass, we let yeast growth to be logistic. We have observed this sort of logistic growth dynamics consistently during our experiments whereby the yeast density saturated after a certain amount of time (Fig 2A, Fig S5A).

A sketch of this model shown in the above figure describes how the growth rate changes as a function of yeast density. At low density, cooperators have a higher growth rate ($\gamma_{C_{low}}$) than cheaters ($\gamma_{D_{low}}$). Above a yeast density N_C where cooperator density is at a critical value, it is assumed that the growth rate is higher for both cooperators and cheaters since glucose accumulates faster in the media[26]. Then, the growth rate decreases logistically to zero as the yeast density reaches its carrying capacity, K. We measured the critical cooperator density at N_C to be about 3 x 10^5 cells/mL and $\gamma_{C_{low}}$ as 0.33 hr^{-1}. These measurements were taken by observing the time it took purely cooperative yeast cultures to reach a certain density, starting with different initial cell densities. Note that N_C is more than two orders of magnitude lower than final cell density that can be achieved by a pure yeast culture in our prepared media over 48 hrs (see K_{max} below). Therefore, we assumed growth rate below this yeast density to be approximately constant (no logistic decline). This assumption can be visualized on the above figure, where below N_C, on a log scale, projections of logistic lines can be taken to be not a function of yeast density as they are nearly constant. In other words, we can ignore the drop in nutrient concentration during the period in which yeast density reaches N_C, as this value is much lower compared to the final yeast density, therefore the nutrient depletion is only a small fraction of the total nutrients present in the media. $\gamma_{C_{high}}$ was measured

to be 0.45 hr^{-1} on 4% sucrose by measuring growth rate during exponential growth. Taking the cost of cooperation into account, $\gamma_{D_{high}}$ was assigned such that $\gamma_{C_{high}}$ was 1% lower than $\gamma_{D_{high}}$ (Figure S1). Highest K value in a pure yeast culture on our default media was measured to be $15x10^7$ cells/mL (K_{max}). To simulate nutrient limitation or competition with bacteria, K was varied across the experimentally observed range.

$\gamma_{D_{low}}$ (cheater growth rate at low density) was treated as a phenomenological parameter and was varied to fit the data shown in figure 3c. In nutrient limitation conditions, cheaters had a growth deficit of 4.85% at low density compared to cooperators. For JM1100 treatment, this deficit was 4.85% + 5.45% * (1- K/K_{max}) and for DH5α it was 4.85% + 13% * (1- K/K_{max}). These values were assigned so as to fit the data. We assumed that cheaters have a lower growth rate than cooperators when competing against bacteria, because bacteria might compete for glucose with yeast and this would further limit the available glucose in the media during low-density conditions (yeast density <N_C). This model enabled us to calculate temporal dynamics and simulate the entire growth process over 5 cycles of growth (10 days) with 1:1,000 serial dilutions in between. Lower carrying capacity due to nutrient limitation or bacterial competition meant that the yeast population would spend more time during the first phase of this growth model where cooperation is favored. According to our model, equilibrium fraction of cooperators without the presence of bacteria is 61%.

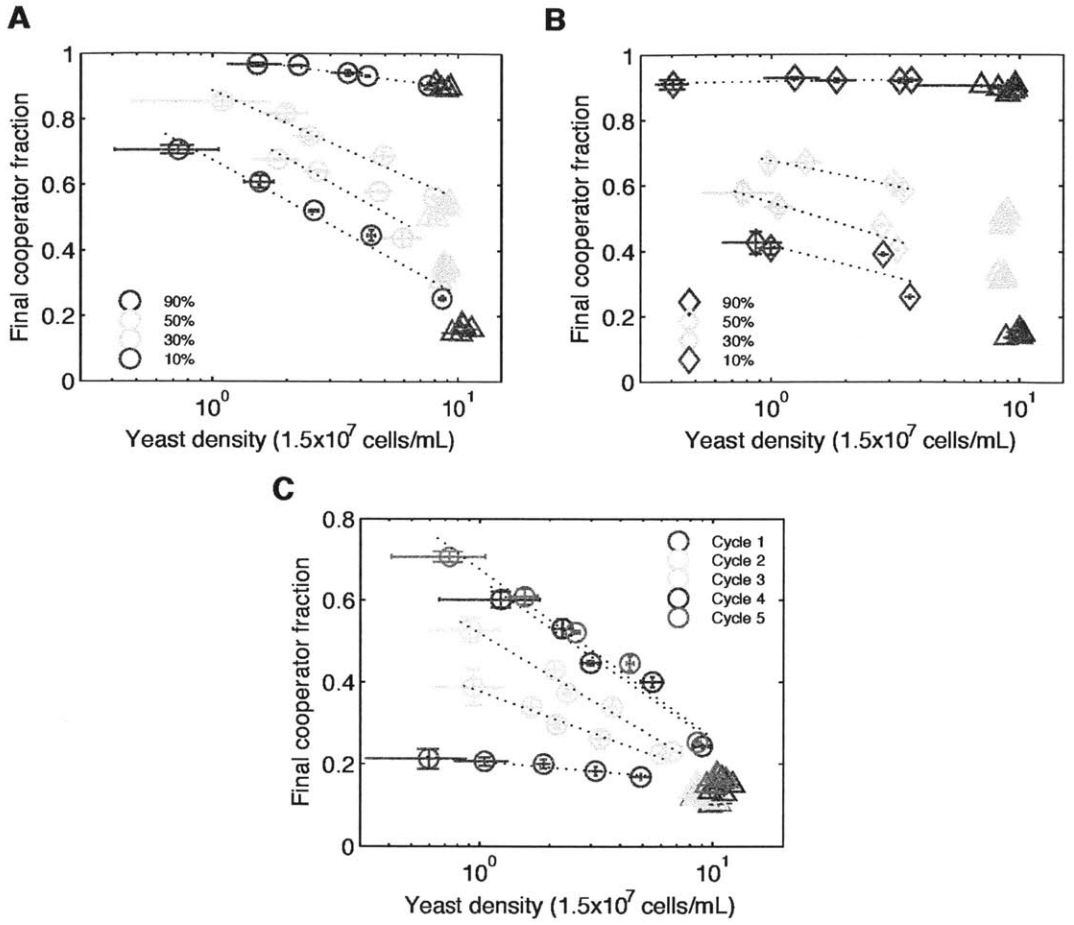

Figure S9: Log-linear relationship between yeast density and final cooperator fraction shown for different initial cooperator fractions (A, B) and different time points during experiments (C). **(A)** Competition results between yeast and DH5α with different initial cooperator fractions (circles) after 5 cycles. **(B)** Competition results between yeast and JM1100 with different initial cooperator fractions (diamonds) after 5 cycles. Triangles represent results for pure yeast cultures both in (A) and (B). **(C)** Final cooperator fraction within the yeast population over time while competing against DH5α. Each cycle is 48 hrs. Data points represent different buffering conditions. Yeast density decreases monotonically with buffering in all the plots above. Note the apparent increase in the final yeast density as the yeast population becomes more cooperative in (C). Dotted lines represent least squares fit for the data. Error bars, ± s.e.m. (n = 3).

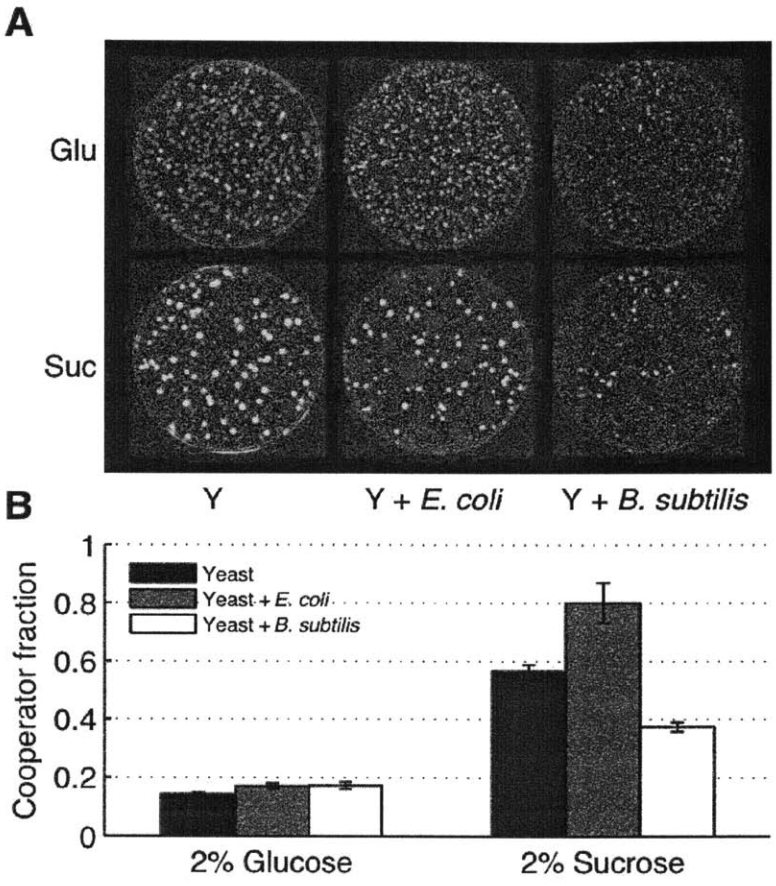

Figure S10: Competition against *E. coli* or *B. subtilis* on agar plates. Growth on agar plates of yeast only, yeast with *E. coli*, and yeast with *B. subtilis* **(A)** Images were taken after 4 days of growth at 30°C. Yeast (Y) was competed against either *E. coli* (JM1100) or *B. subtilis* on rich media plates (100mm diameter) supplemented with either 2% Glucose or 2% Sucrose. Cooperator yeast colonies appear yellow/green, cheater yeast colonies appear red and bacterial colonies appear dull colored and bigger compared to yeast colonies. **(B)** Colonies were washed off of imaged plates and yeast cooperator fractions were measured by flow cytometry. As expected, competition with *E. coli* selected for cooperators within yeast. In contrast, *B. subtilis* favored cheating. Error bars, ± s.e.m. (n = 3).

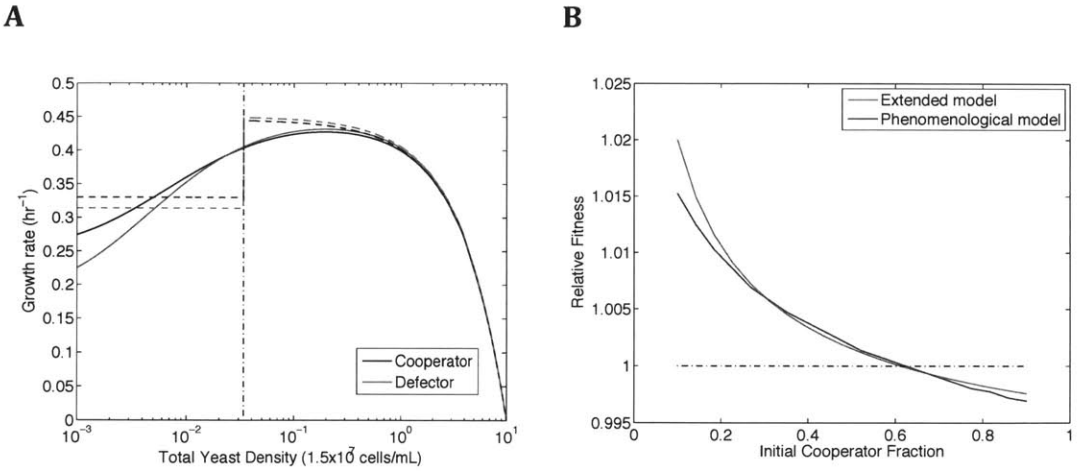

Figure S11: A detailed yeast growth model produces similar results as our phenomenological model: To show that our phenomenological model (Figure S8) can predict yeast growth dynamics accurately, we developed a logistic growth model incorporating glucose production by cooperator cells. In this extended model, the growth rates of cooperators (γ_C) and defectors (γ_D) were assumed to follow Monod-like dynamics as a function of the glucose concentration together with logistic growth at high cell density:

$$\gamma_C = \gamma_{C_0}\left(1-\frac{N}{K}\right)\cdot\left(\frac{G+g}{G+g+K_m}\right)$$

$$\gamma_D = \gamma_{D_0}\left(1-\frac{N}{K}\right)\left(\frac{G}{G+K_m}\right)$$

Here, γ_{D_0} is 0.45 hr^{-1} and γ_{C_0} is 0.99x0.45 hr^{-1} corresponding to the 1% fitness cost of producing invertase as used in the phenomenological model. N is the varying total yeast density during a batch culture and K (15x10^7 cells/mL) is the carrying capacity of the yeast population. Growth rate of yeast cells is assumed to be a function of G (which denotes the glucose concentration (%) in the media) with Michaelis-Menten (Monod) dynamics, where K_m is 0.005% to yield an approximately correct growth rate at low cell density. However, we note that previous measurements suggest that the growth rate saturates more rapidly with increasing glucose concentration than is assumed in the Monod / Michaelis-Menten form above (Gore et al, 2009). Initial G concentration is set to be 0.005%, as in our experiments. g denotes the small

amount of glucose concentration felt and captured directly by the cooperator cells. g was set to be 0.003% as described in Gore et al.

We modeled the glucose production to be proportional to the cooperator cell density:

$$\frac{dG(\%)}{dt} = \frac{Cooperator\ density\left(\frac{cells}{L}\right) x\ 4.5x10^{8}\left(\frac{molecules}{\sec x\ cell}\right)}{N_A} x\ 180(\frac{g}{mol})\ x\ 0.1$$

Time step (dt) used in the simulations is 1 sec. Based on our previous measurements, we set the sucrose hydrolysis rate to be $4.5x10^{8}\left(\frac{molecules}{\sec x\ cell}\right)$ (Gore et al 2009). In this model we only explicitly consider glucose creation (not glucose consumption), as the primary dynamics between the cooperator and cheater yeast strains are determined by the glucose concentration at low cell density. As the cell density increases glucose and other resources will be exhausted, which is what leads to the logistic slow-down of cell division at high cell density. N_A is the Avagadro's number and 180 g/mol is the molecular weight of glucose. We multiply by 0.1 to convert g/L into % (w/v) concentration.

Using this model, we simulated the growth dynamics of mixed yeast cultures and compared the results to the predictions of our phenomenological model. (A) We found that growth rates of yeast strains as a function of yeast cell density behave qualitatively very similar to the phenomenological model. Moreover, we found that after a critical cooperator cell density, the cheater growth rate exceeds the cooperator growth rate, although at low-density conditions the cooperator growth rate is higher. This critical density was almost exactly the same for the extended model as the one used in our phenomenological model. For the parameters of the phenomenological model, we used exactly the same values given in Figure S8 (e.g. critical cooperator density was 3 x 10^5 cells/mL, cheater growth deficit at low density conditions was 4.85%). Starting cell densities were 1.5x10^5 cells/mL and initial cooperator fraction was 60% for the plots in (A).

Next, we simulated cultures with different starting cooperator fractions and plotted the relative fitness of cooperators as a function of starting cooperator frequency (B). We found that the results of the extended model were almost identical to the phenomenological model and both models predicted the equilibrium fraction of cooperators to be around ~60%. For these simulations, we used an initial yeast density of 1.5×10^6 cells/mL (equilibrium density during experiments with 1000x dilution). The relative fitness was calculated using the formula given in Figure S1. These results show that although simple, our phenomenological model captures the essential dynamics of yeast growth on sucrose accurately. In our simulations, by decreasing the initial glucose concentration, we can indeed drive the equilibrium fraction of cooperators to 1 (occurs at initial glucose concentration of ~0.001%). This result shows that glucose consumption due to the presence of bacteria would drive the increase in cooperator fractions in this model.

In this mechanistic model we have attempted to use experimentally measured parameters together with well-known growth equations (i.e. Monod), meaning that the growth rates at low cell density are different in the mechanistic model and in our phenomenological model. Nevertheless, the primary argument that we are attempting to make here is that a mechanistic model which explicitly treats glucose concentration will yield similar predictions regarding cooperation/cheating as our phenomenological model that simply has two-phases of growth corresponding to low and high cell density. Figure S11B above argues strongly that the two modeling approaches make similar predictions.

PART II

Evolutionary outcomes in community structure across replicate ecosystems

Experiments to date probing adaptive evolution have predominantly focused on studying a single species or a pair of species in isolation. In nature, on the other hand, species evolve within complex communities, interacting and competing with many other species. It is unclear how reproducible or predictable adaptive evolution is within the context of a multispecies ecosystem. To explore this problem, we let many replicates of a multispecies laboratory bacterial ecosystem evolve in parallel for hundreds of generations. We found that after evolution, relative abundances of individual species varied greatly across the evolved ecosystems and that the final profile of species frequencies within replicates clustered into several distinct types, as opposed to being randomly dispersed across the frequency space or converging fully. By substituting individual evolved species back into the ancestral community we demonstrated that these divergent community structure patterns were driven by specific species adapting exceptionally well in each community structure state. Our results suggest that community structure evolution has a tendency to follow one of only a few distinct paths.

INTRODUCTION

Although research is abound focusing on the adaptive evolution of a single species or a pair of interacting species, the problem of how evolutionary processes shape a complex natural ecosystem has received less attention [50]. Given the initial biotic and abiotic components of an ecosystem, it is not obvious whether we can ever predict the future community structure and species distribution for that ecosystem [51]. Resolving this challenging problem about community evolution is not only important from an intellectual standpoint, but also has implications for our ability to forecast the evolutionary responses of ecosystems to recent anthropogenic pressures [52].

Traditionally, research has pointed to character displacement, whereby co-occurring similar species diverge in their adaptations, and co-evolution as mechanisms to explain and predict adaptation in simple communities [51]. However, recent theory and experiments suggest that such predictions from niche occupancy patterns or pairwise species interactions often fail to predict adaptive evolution in more complex ecosystems composed of more than two species [53,54]. For instance, a recent experimental study with microbes found that community complexity can greatly alter adaptive evolution in a way that is not obvious from single species evolution [55]. Diffuse coevolution studies have also found evidence that coevolution of a focal pair of interacting species can be influenced by the presence of other species [54,56].

All of these and similar studies mainly strive to elucidate deterministic mechanisms for multispecies adaptive evolution. However, we may also ask, to what degree is there randomness in the path that a multispecies ecosystem follows through adaptive evolution? If we could replay the evolution in a closed community many times starting from the same initial state, would we always end up in the same final state with the same abundances and kinds of species? Or would we get a different result each time? Recent theoretical and empirical studies using a single species suggest that adaptive diversification can be a surprisingly deterministic evolutionary process [57,58]. However, how this relates to multispecies adaptive evolution is less clear [51].

To address this problem, here we present experiments probing the adaptive evolution of a multispecies model community. We found evidence that the adaptive evolution of this experimental community is not deterministic, yet at the same time is not completely random. Our model community consisted of six soil bacteria species spanning three different genera: *Enterobacter aerogenes* (EA), *Serratia marcescens* (SM), *Pseudomonas fluorescens* (PF), *Pseudomonas aurantiaca* (PA), *Pseudomonas veronii* (PV) and *Pseudomonas putida* (PP). We let this community evolve in a complex environment containing dozens of carbon sources that can be

found in soil (see methods)[59]. We chose the species on the criteria that they could grow together in our media without aggressively antagonizing each other via either predation or expression of anti-microbial compounds. The carbon utilization profiles for these species were not completely overlapping, but also not fully orthogonal (Fig S1). Compared to natural ecosystems with complex trophic levels and numerous types of species interactions, our model ecosystem is a simple one, where we expect most of the interactions between species to be driven by competition for resources [60].

RESULTS

We began by characterizing the relative abundance of the six bacterial species when mixed together. We prepared 96 identical ecosystems containing all six species, which we will refer to as the ancestral communities. We then allowed these ecosystems to reach (short-term) equilibrium by propagating through four growth dilution cycles. Each cycle of growth was 48 hours without shaking and the dilution was by 1,500, corresponding to approximately 10.5 cellular divisions per cycle. We were able to quantify the final species abundance by plating the communities on solid agar media and counting the colony numbers for each species, as each species had a unique colony color/morphology (Fig 1A). We found that *Pseudomonas putida* (PP) quickly fell to less than 1% abundance, whereas the other species were all between 15 – 35% in frequency. This coexistence of five of the six bacterial strains was observed in all 96 of our replicate ecosystems, suggesting that the short-term equilibrium of this ecosystem is reproducible and robust to experimental procedures and errors in measurement.

Next, we performed a long-term evolution experiment consisting of 96 identical replicates of the six species community and let these evolve in parallel for ~400 generations, which we call the "multispecies evolution" treatment (Fig 1B). At the end of the experiment, we measured the final community structures (i.e. the relative abundance of each species) in all communities. We found that all species except PP were very robustly coexisting in all of the replicate ecosystems. Surprisingly, in 9

out of the 96 ecosystems *Pseudomonas putida* (PP) not only survived the multispecies evolution process, but came to dominate the resulting communities (mean frequency of ~25%). This stark bimodality in survival probability observed with PP may be due to a rare mutational event that rarely occurred before PP went extinct.

In addition to evolution of the multispecies ecosystems, we in parallel performed isolated evolution of each of the individual species constituting this multispecies community ("isolated evolution"). The isolated evolution treatment was designed to tease apart whether multispecies evolution was in any way different from the case where each species would evolve purely in response to the abiotic environment, irrespective of the presence of other species. For this, we let six replicates of each species evolve in isolation, in parallel with the multispecies treatment. After the long-term evolution experiment was over, we consolidated 96 multispecies communities by using the species from the isolated treatment (see methods). These new communities were grown for several cycles to reach equilibrium, after which we measured the final community structure by plating as we did for the multispecies treatment (Figure 1B). Similar to the results with the ancestral communities, the newly generated communities using the isolated evolution lines yielded coexistence of species EA, SM, PF, PA and PV. Again, PP was going extinct or may be surviving only below 1% in frequency after a few cycles of growth in all communities (see methods).

Focusing on the mean abundances from the two treatments, the most striking difference was that the abundance of PV was significantly lower in the isolated treatment compared to both the multispecies and the ancestral treatment (Fig 2A). The outcome of evolution in this new environment was therefore different depending upon whether the species were co-evolving or evolving in isolation, in line with previous experimental results in a different microbial ecosystem [55].

A second notable feature of the relative abundance data was that PF was more abundant in the multispecies and isolated treatments than in the ancestral community, which might be due to some inherent advantage that this species possesses in terms of being able to adapt to this new environment. We also note that although we measure relative abundances (frequencies) of species in our experiments, these measurements can also be taken as a proxy for absolute abundance, since we did not observe any significant differences in final community productivity/optical density across treatments and replicates within each treatment (Fig S2).

The level of variation in relative species abundances across replicate communities also differed across the three treatments (Figure 2A). Variation in species frequencies in the ancestral communities was much lower in comparison with the isolated and multispecies treatments, consistent with the expectation that adaptive evolution would increase community structure variation. Given that ancestral replicates were identical and had no time to evolve, variation in this treatment can be treated as a sum of measurement error and intrinsic fluctuations in the community structure. Therefore, by looking at the variation in the ancestral treatment, we can get a measure of this base error rate (Figure 2A, Interquartile range: 6-8%). We also measured the beta diversity of each treatment as another measure of variation (Jenson-Shannon divergence). We found that the multispecies treatment had a considerably higher beta diversity compared to both isolated and ancestral treatments (Fig 2B).

As discussed previously, PP went extinct in most of the multispecies community replicates (86/96; see figure 2C), but when it survived came to dominate the community. This conclusion is also apparent looking at the raw frequency data plotted for each treatment (Figure 2C). PP dominance is unique to the multispecies treatment, since in both ancestral and isolated treatments, we did not have any PP penetration to this degree.

So far, we observed variation in community structure after adaptive evolution in multispecies and isolated treatments, and significantly more so in multispecies treatment. It is also important to determine whether there is anything deterministic about this variation. For instance, do the final community structures across replicates cluster into distinct types, where some fraction of the replicates converges onto the same community structure? If true, is there anything different between the treatments in terms of the cluster types and frequencies that we observe? To this end, we performed cluster analysis on our relative abundance data. We used consensus clustering, which provides quantitative and visual stability evidence for estimating the number of unsupervised classes in a dataset [61]. Briefly, consensus clustering involves repeated subsampling of the data and then applying a clustering algorithm to each subsample (see methods). In the case where there are very distinct clusters in the data, an observation in each subsample would always cluster with the same set of observations regardless of which portion of the whole dataset we are using. Alternatively, if the clusters were not robust depending on the subsample then the cluster assignment for each observation would vary. The "consensus" score of two observations is essentially the frequency with which they cluster together. This score would be 1 if the two observations always clustered into same class in each subsample where they happened to be both present.

A clustering analysis of the relative species abundances from the multispecies evolution experiment argued that our 96 replicates can be divided into four distinct outcomes (Figure 3A). Visual inspection of the heat maps of consensus score matrices for different k's (number of clusters) suggests that the most clean matrix is for k=4, indicating that the optimal number of classes in this dataset is 4 (for a more detailed analysis, see fig S3). We also performed the same clustering analysis for the isolated evolution treatment, which indicated that the optimal clustering of this data is in two classes (Fig 3B, fig S4). The same analysis was performed for a randomly generated dataset and the ancestral dataset. The results from these analyses showed that multispecies treatment has a comparably higher clustering quality and larger number of distinct clusters (Fig S5-S6).

We further evaluated the quality of clustering by looking at the mean cluster consensus for each treatment, where we took the mean of the average consensus scores for each cluster identified. We observed that mean cluster consensus values for both the ancestral and random datasets were lower compared to multispecies and isolated treatments, random dataset being the least robust overall (Fig S7A). We also confirmed that our results were robust to the clustering method used, as similar cluster quality and number trends were observed with hierarchical clustering of the same data (Fig S7B).

Taken together these results suggest that adaptive evolution in our experimental system often resulted in one of several distinct community structure states in multispecies and isolated treatments, more so than would be expected by random variation. Moreover, multispecies treatment resulted in higher number of these states/clusters compared to the isolated treatment, suggesting that multispecies adaptive evolution might be less predictable compared to single species evolution. This result is also consistent with the high beta diversity observed in the multispecies dataset.

Next, we wanted to understand the underlying mechanisms leading to this clustering effect. To address this question, we compared each cluster to the ancestral community structure (Fig 4A). We quickly realized that each cluster was mostly defined by one single species doing significantly better compared to its counterpart in the ancestral community. The most extreme example of this occurred in cluster 1, where PP was present in very high frequency whereas it was practically extinct in the ancestral community. We observed similar shifts in frequency in other clusters, yet the species that seemed to be doing better was different in each case. In cluster 2, EA was higher compared to its level in the ancestral community. PV and PF had higher relative abundance in cluster 3 and 4 respectively. Given this observation, we hypothesized that the behavior of each cluster could be mainly

driven by only one species (PP, EA, PV or PF) increasing in frequency, probably owing to a relatively rare mutation conferring a significant selective advantage.

To test this hypothesis, we collected isolates for each species from each cluster in the multispecies treatment (4 randomly chosen communities per cluster and 3-5 pooled colonies per species in each community, giving 4 clusters x 4 communities x 5 species = 80 isolates plus 4 PP isolates from cluster 1, totaling 84 isolates). We then systematically created communities where each evolved isolate replaced its counterpart species in the ancestral community (84 communities corresponding to 84 isolates from evolved communities). We then grew these communities to equilibrium and measured relative abundances.

A principal component analysis (PCA) of the resulting species abundances was consistent with our hypothesis that the clusters were largely driven by adaptive evolution of the common species from each cluster. Given this hypothesis, we expected to see clusters in PCA plots due to the possibly distinct behavior of communities assembled with isolates we thought were driving the behavior of each cluster (eg PP from cluster 1, EA from cluster 2 etc). Indeed, we found that communities assembled with PP isolates from cluster 1, EA isolates from cluster 2 or PF isolates from cluster 4 had distinct community structures and clustered separately in PCA plots (big circles in fig 4B). However, we did not observe a separate cluster corresponding to communities prepared with PV isolates from cluster 3. When we compared all the communities excluding the ones assembled with our hypothesized isolates (big circles in fig 4B) against the ancestral community structure, we found that there was little difference (fig 4C). The only exceptions were that communities with PF or PV isolates did in general have higher PF or PV frequencies respectively, compared with the ancestral community. This observation suggests that in all the clusters there might be across the board adaptation within the context of certain species.

Finally, we compared the ancestral communities assembled with our hypothesized isolates (PP from cluster 1, EA from cluster 2, PV from cluster 3, PF from cluster 4) with the evolved clusters and the original ancestral community. We found that we could reproduce the qualitative behavior of each cluster observed in multispecies treatment (Fig 4D). In conclusion, these results suggest that the significant clustering we observed was the result of a single species gaining an advantage and increasing in frequency in each cluster. This strong effect seemed to produce divergent states in the community structure across replicates, because in each distinct outcome a different species was more abundant.

DISCUSSION

Here we developed an experimental model ecosystem that exhibits robust coexistence of 5-6 soil bacteria species. This system allowed us to perform highly parallel long-term co-evolution experiments. In the end, we found that although there is variation in the final outcome of adaptive community evolution, the final community structure seems to end up in one of a few distinct states. Moreover, these final states depend on whether the evolution occurred in a multispecies community or as isolated single species, suggesting that multispecies ecosystem evolution is fundamentally different from species evolving by themselves. We found that the discreet states we observed after multispecies evolution are the result of a different species doing substantially better than others in each case. It would be interesting to probe even longer term co-evolution, as the "final" ecological states that we have examined here are of course simply a snapshot in time of the co-evolutionary process.

We can ask whether the large changes in community structure that we observed are really due to evolution as opposed to being manifestations of different stable ecological states. Firstly, if this were true, we would expect to observe such variation in ancestral communities or consolidated isolated lines. Instead, ancestral communities displayed no significant clustering or variation and the isolated treatment had only two clusters compared to the four observed in the multispecies

treatment. These results are also in line with our repeated observations with ancestral lines where, independent of the initial inoculation frequencies of the species, the measured community structures were invariably the same after a few cycles of transfers. Moreover, replacement experiments showed that by using isolates from evolved communities, we could reproduce the community structures observed at the end of the evolution experiment, suggesting that the changes in community structure were driven by evolutionary responses rather than stochastic fluctuations.

The predictability of adaptive evolution is a fundamental question that has puzzled evolutionary biologists since Darwin[62]. Studies investigating the determinism of adaptive evolution have historically focused on adaptive radiation of single species into new environments. For instance, more than a decade ago, researchers reported that replicated adaptive radiations of island lizards indicate that adaptive radiation follows deterministic paths resulting in convergent evolution[63]. Since then, subsequent studies using lizards or other animals have reinforced these results [64–67]. In addition to such animal studies, microcosm experiments have also pointed to similar conclusions. Evolution experiments using organisms like *E. coli* or viral models found evidence of parallel evolution, whereby replicate populations evolved convergent characteristics when adapting to new environments [58,68–71]. Similarly, instances of parallel evolution have also been observed among higher organisms like plants and insects and also in nematode development [72–75]. These studies suggest that at least within the context of a single species, evolution can be surprisingly deterministic and convergent.

In contrast to these previous studies, our experiments looked at adaptive evolution of a multispecies community rather than focusing on a single species. We found that this multispecies aspect can result in a less predictable outcome of adaptive evolution than single species studies would suggest. Even without external perturbations or environmental fluctuations, we observed intrinsic randomness in evolution that comes with having a multispecies ecosystem. Nevertheless, we still

found that the adaptive community evolution is not completely random and final community structures cluster into several distinct types. However, more laboratory experiments and data from wild populations are needed to validate the generality of our results. Experiments using tractable multispecies ecosystems like ours can improve our understanding of the predictability of community structure evolution.

MATERIALS AND METHODS

Species and media

The six soil bacteria species we used were *Enterobacter aerogenes* (ATCC#13048), *Serratia marcescens* (ATCC#13880), *Pseudomonas fluorescens* (ATCC#13525), *Pseudomonas aurantiaca* (ATCC#33663), *Pseudomonas veronii* (ATCC#700474) and *Pseudomonas putida* (ATCC#12633), and they all were obtained from ATCC. The growth media was prepared using commercially available BIOLOG EcoPlates. These microplates contain 31 different carbon sources useful for soil community analysis. In addition to these carbon sources, in each well there is a tetrazolium dye (5 cyano-2,3 ditolyl tetrazolium chloride), which is reduced to a violet-fluorescent formazan molecule, when the carbon source is oxidized by the cells. The color development was measured by light absorption at 590nm, which quantified the productivity of cultures. At the same time, the optical density of the cultures was measured at 750nm, where the tetrazolium dye is not absorbent. Our base media was M9 minimal media, which contained 1X M9 salts (Sigma Aldrich), 2mM MgSO4, 0.1 mM CaCl2, 1X trace metals (Teknova). We filled the EcoPlate by adding 140uL of this base media into each well and let the lyophilized carbon sources dissolve for 30 min. Then, we mixed all the contents of the wells (except the blanks) to get a complex medium containing all of the 31 carbon sources. For initial inoculation and growth of the species before experiments, we used nutrient broth (0.3% yeast extract, 0.5% peptone). We used nutrient agar plates (nutrient broth + 1.5% agar) to count colonies and measure the relative abundances of species. All experiments were done at 24C.

Evolution experiment

From frozen stocks of ancestral lines, we directly inoculated each species separately into nutrient broth and let them grow for 48 hrs in loose cap culture tubes without shaking. Next, we inoculated the grown cultures into our base media and again let the species grow separately for two cycles of transfers (48 hrs each). We diluted these by 1/100 into M9 minimal media (w/o carbon sources) then added 10 uL of this mixture onto 140 uL of our base media corresponding to 1/1500 dilution in total. These cultures were inoculated into flat bottom 96 well plates, every well of the microplate contained 150 uL of media plus cells. For each transfer, we diluted cultures by 1/1500 into freshly prepared media. After this initial period of growth, we made frozen stocks of these cultures and at the same time we initiated the two treatments of the long-term evolution experiment: (1) For the multispecies treatment, we diluted each of the individual species by 1/100 and then mixed them by equal volume. After this, we diluted that mixture by 1/15 into freshly prepared base media and then used this final mixture to inoculate the wells. We had 96 replicates for this treatment, and these replicates were spread over two 96 well plates using a checkerboard pattern to mitigate risk of cross-contamination. (2) For the isolated treatment, we diluted those same cultures for the individual species by 1/1500 and had 8 replicates for each species adding up to 48 cultures in total for six species. These were also spread over a 96 well plate in a checkerboard pattern. Throughout the course of the evolution experiment, every 48 hrs, cultures in both treatments were diluted by 1/1500 into media that were freshly prepared just before the experiment. The cultures were incubated without orbital shaking.

Measurements after the evolution experiment

After 42 cycles of transfers, we measured the relative abundances in the multispecies treatment by plating on nutrient agar plates. For each replicate, we diluted the final cultures by $1/10^6$ in phosphate buffered saline, and plated 75uL of this solution onto an agar plate. We plated each replicate twice, as during preliminary experiments, we found that there was large variation in the total number of colonies that showed up on plates. After 48 hrs, we counted all the colonies on two plates together to measure the relative species abundances. For

each replicate at least ~90 colonies were counted. We also plated all 48 cultures in the isolated evolution treatment to check for possible contamination. We found that 2 replicates of one of the species (PA) had no colonies on agar plates possibly due to external contamination. We discarded these replicates and used the remaining ones. We also made frozen stocks for all of these final cultures.

To prepare the consolidated communities for the isolated treatment, we randomly chose 6 of the replicates from 8 replicates for each species. We chose 6 to balance out the fact that we had only 6 viable replicates for one of the species (PA). Next, after inoculation into base media from frozen cultures and growth for two cycles, we randomly chose a replicate from the 6 replicates for each species and mixed them equally by volume then repeated this process for 96 times to get 96 randomly consolidated communities using the species from the isolated evolution. We diluted these communities by 1/1500 into fresh media and let them grow for 4 cycles of transfers after which we plated them and measured the relative species abundances as we have done for the multispecies treatment. We found that 4 of these cultures had no growth in the end so we used the 92 remaining for our measurements. We got visible PP survival only in 3 of the communities but in very low abundance (~1%, 1 colony in ~100). To see if this was due to the initial mixing ratios we had used, we repeated consolidation again using the same procedure of random mixing but this time instead of using 1/6 of volume for PP, we used a proportionately excess amount of 1/4 in volume while the other species equally occupied the other 3/4. After 4 cycles of growth, PP was visible only in 6 communities but was still less than 3% in frequency. We decided to use the initial dataset where we had initially mixed all the species by equal volume, as there was no appreciable effect of increasing the initial frequency of PP. For preparing the ancestral communities, we revived the frozen stocks of ancestral species that were stored during the initiation of the evolution experiment and let them grow in base media for 2 cycles then mixed them by equal volume, and created 96 replicate communities. After 4 cycles of transfers of these communities, we plated them and measured relative species abundances. PP colonies were found in 4 communities, but we could count only one

or two colonies per plating in all of these cases. We did not observe any significant difference in community structure with or without PP either for ancestral communities or for the communities created using isolated lines (data not shown). Therefore, for our analyses with the ancestral and isolated treatments, we assume that PP is essentially extinct and exclude PP data, also taking into account that these low frequency measurements could be false positives. We also note that our measurement resolution was not sufficient enough to measure frequencies lower than ~1% but PP could still be surviving in lower frequencies in these experiments albeit not detectable by our measurements.

Cluster analysis

For consensus clustering, we used k-means clustering algorithm with Pearson distance. 80% of the data was subsampled without replacement for a total of 100 iterations. This process was repeated for each k (number of clusters) and the results from these were used these to create consensus matrices and calculate mean consensus values for each class and each observation in the dataset. Items or clusters were not weighted in the subsamples. We generated a random dataset by creating 96 artificial observations, where each observation contained five frequency variables, as in our actual relative abundance datasets. These frequency values were assigned by drawing from a uniform distribution and then normalizing across each observation. Having six frequency variables instead of five did not change the results. Hierarchical clustering was performed using Euclidean distance and 'ward' linkage. Calinski-Harabasz index is a measure of the ratio of inter-cluster variation to within cluster variation, hence the larger this number is the better the cluster separation and cluster compactness. These analyses were performed using R statistical language and open source packages [61,76].

Replacement experiments

At the end of the evolution experiment we froze all the communities as mentioned previously. To perform the replacement experiments, for each identified cluster in the multispecies treatment, we inoculated 4 randomly selected communities into

fresh media from the frozen stocks (4x4 = 16 communities). We propagated these cultures for 4 cycles of transfers using the same scheme we had in the long-term evolution experiment. Then, we plated these 16 communities and picked 3-5 colonies per species from each plate. We pooled the picked colonies for a given species from a plated community and then inoculated those into fresh media (5 species per plate from clusters 2,3,4; and 6 species per plate from cluster 1, i.e. 3 clusters x 4 communities x 5 species = 60 isolates in total from clusters 2,3,4; plus 1 cluster x 4 communities x 6 species = 24 isolates from cluster 4). We let these isolates grow for 2 cycles. For the replacement experiment, we mixed each isolate with its complementary ancestral species (which were also grown for 2 cycles in parallel with isolates). For instance, for an EA isolate, we mixed it with ancestral species SM, PF, PA, PV. We again let these newly prepared communities grow for 4 cycles of transfers before we plated them to measure relative abundances.

FIGURES

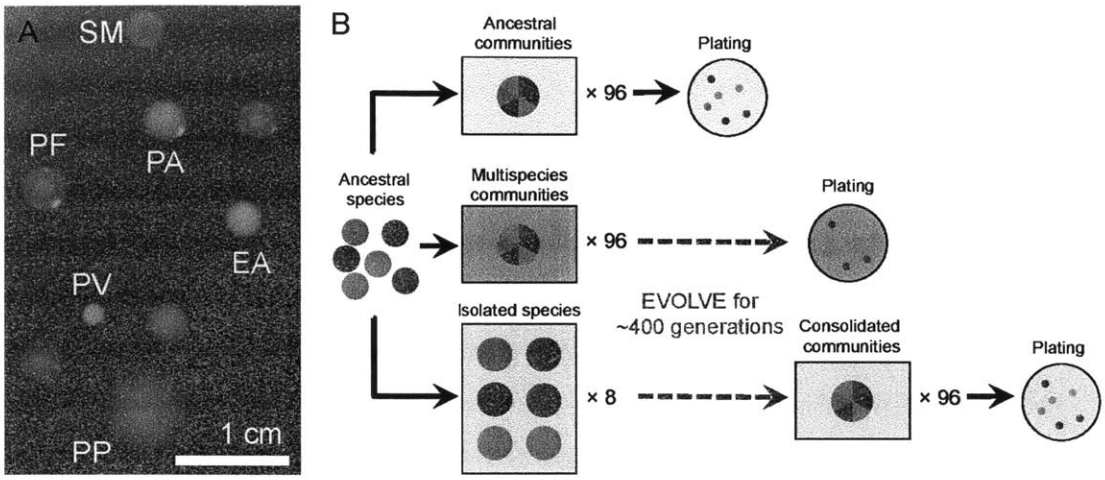

Figure 1: Species appearance on an agar plate and evolution experiment design (A) A photograph of colonies of all six species spread plated on an agar plate. Note the distinct colors and sizes of colonies, which enabled us to distinguish between the species (EA: *Enterobacter aerogenes*, SM: *Serratia marcescens*, PF: *Pseudomonas fluorescens*, PA: *Pseudomonas aurantiaca*, PV: *Pseudomonas veronii* and PP: *Pseudomonas putida*). **(B)** This schematic shows the different treatments of the evolution experiment and how they were prepared. Ancestral species were mixed to create ancestral communities. For the multispecies treatment, again ancestral species were mixed together to establish 96 identical multispecies communities, but this time they were propagated as part of the long term evolution experiment. For the isolated treatment, ancestral species were inoculated separately to create "isolated" lines with 8 replicates for each species and propagated along with the multispecies treatment. These long term evolution treatments were propagated for ~400 generations corresponding to 42 cycles of transfers into fresh media every 48 hours. In the end, multispecies communities were plated to measure relative abundance of species in each of the 96 replicates. Isolated lines were consolidated to make 96 multispecies communities. These consolidated communities from isolated lines were propagated for a short time and then plated for measurements.

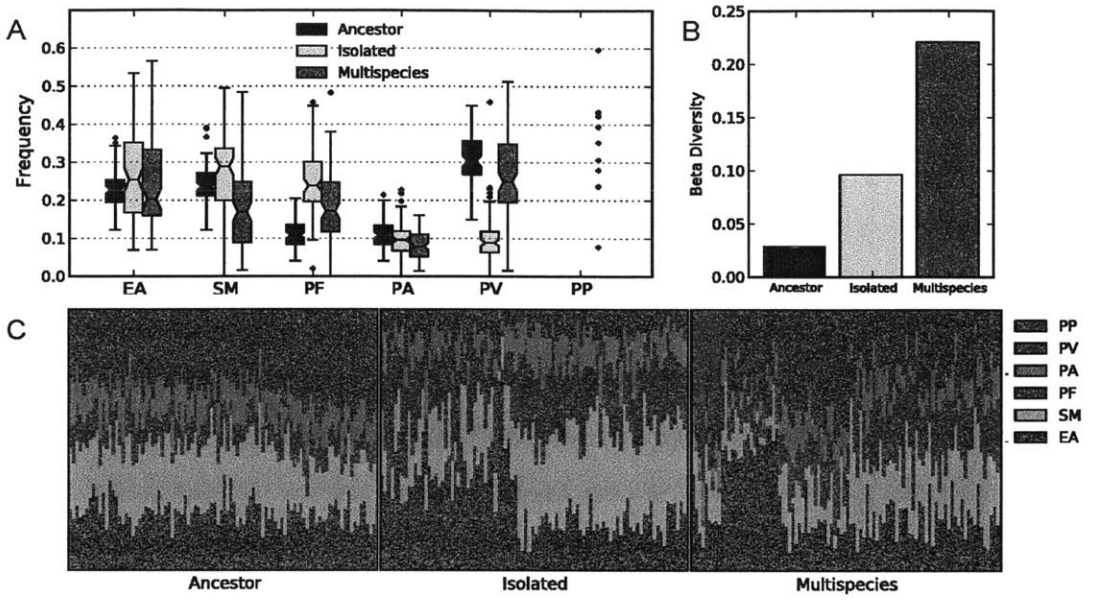

Figure 2: Community structure outcomes look different across evolutionary treatments (A) Box plots of relative abundance of each species for the replicates of different treatments. Note the 10 outliers in multispecies treatment for PP **(B)** Beta diversity for different treatments, calculated using Jensen-Shannon divergence. Bars represent mean of 1000 bootstrap runs with sample size 96 (with replacement), error bars too small to be visible (<1e-15) **(C)** Stacked area plots of raw relative abundance data for ancestral, isolated and multispecies treatments. Data is clustered and ordered using a hierarchical clustering algorithm to aid with visualization of distinct community structures. Horizontal axes represent observations (Ancestor: 96 samples, cluster # k=2; Isolated: 92 samples, k=2; Multispecies: 96 samples, k=4).

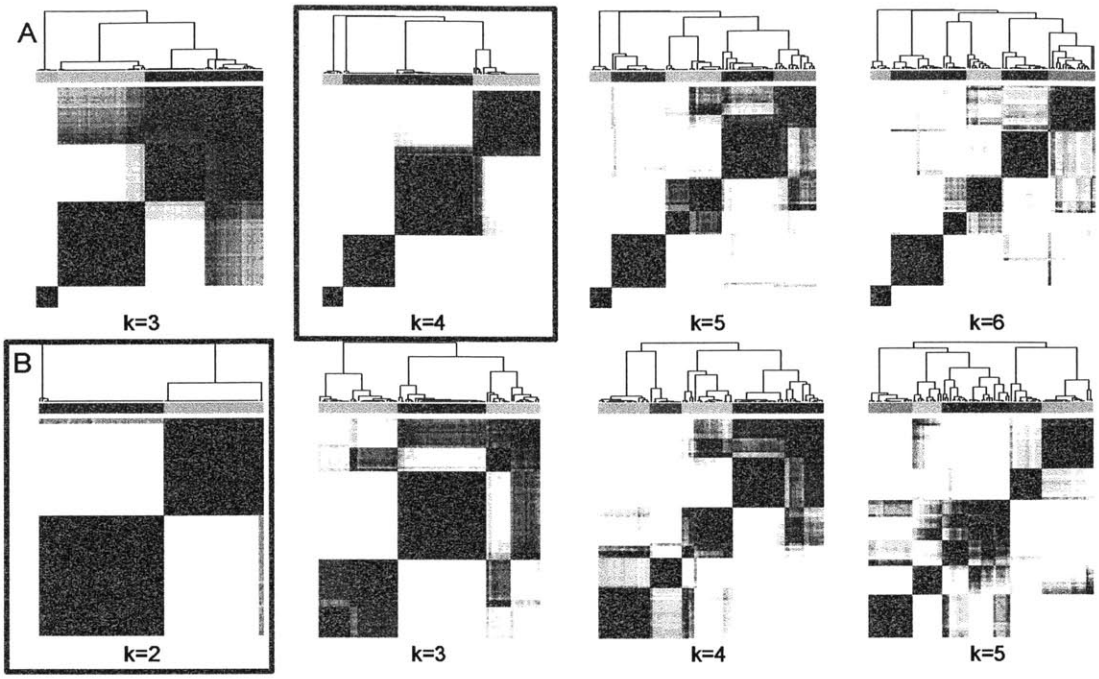

Figure 3: Multispecies treatment results in higher number of distinct community structures as quantified by consensus clustering (A) Consensus matrices for multispecies treatment. **(B)** Consensus matrices for isolated treatment. k values indicate number of clusters used in k-means algorithm. Rows and columns correspond to observations. Note that the cleanest matrix for multispecies treatment is at k = 4, whereas for the isolated treatment it is at k = 2 (indicated by big squares). Consensus values range between 0 and 1, colored by white to dark blue. Scaling is the same across all plots. A consensus value of 1 for two items means these two items clustered together 100% of the time across all subsamples, whereas a value of 0 means that two items never clustered together (see methods). A dendrogram of consensus clustering results is plotted above the columns of the heat maps, and the identified clusters are color coded.

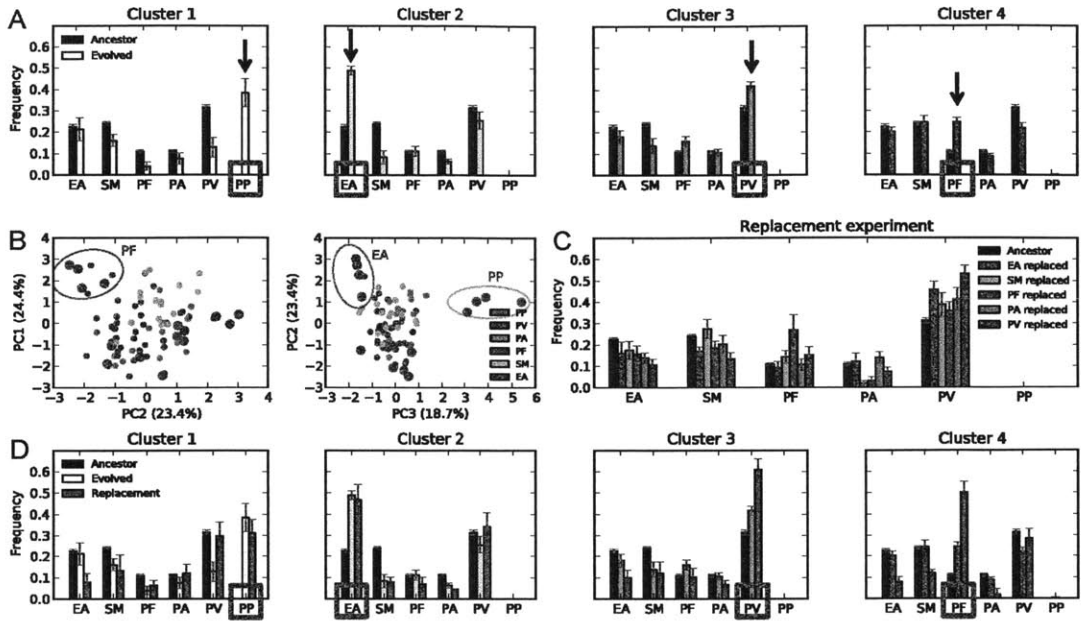

Figure 4: Replacing ancestral species with evolved isolates in the ancestral community reproduces the clustering behavior (A) Comparison of each cluster against ancestral community (n = 9 for cluster 1, n = 18 for cluster 2, n = 22 for cluster 3, n= 47 for cluster 4. Species that are significantly higher in frequency compared to their ancestral level are indicated with arrows. **(B)** Principal component analysis (PCA) plots for replacement experiment data. Each circle represents an ancestral community in which a species is replaced with an evolved isolate from the multispecies treatment. Circles are color-coded based on the species that is replaced in the ancestral community. Big circles represent communities in which ancestral species are replaced with evolved isolates that were highlighted in (A) **(C)** Mean relative abundance for the communities shown in PCA analysis in (B), excluding big circles. **(D)** Comparison of each cluster against ancestral community and the communities created by replacement with the hypothesized species from (A) (big circles in B). Replaced species are highlighted in squares on the x-axis labels, error bars are 95% confidence interval around mean.

SUPPLEMENTARY FIGURES

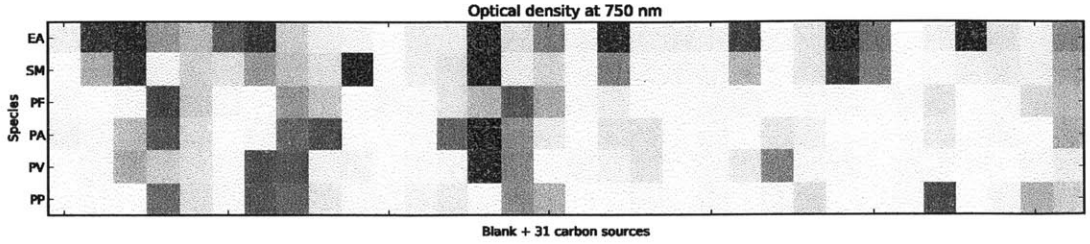

Figure S1: Carbon utilization profiles. Heat map of productivity measurements (OD @ 750 nm) for each species on 31 different carbon sources present in the Biolog EcoPlate (see methods). Each square represents final productivity measurement after 48 hours of growth on an individual carbon source. Leftmost column is blank (no carbon source). White represents no growth, with darker squares indicating higher growth. Color scale is the same across all heat maps.

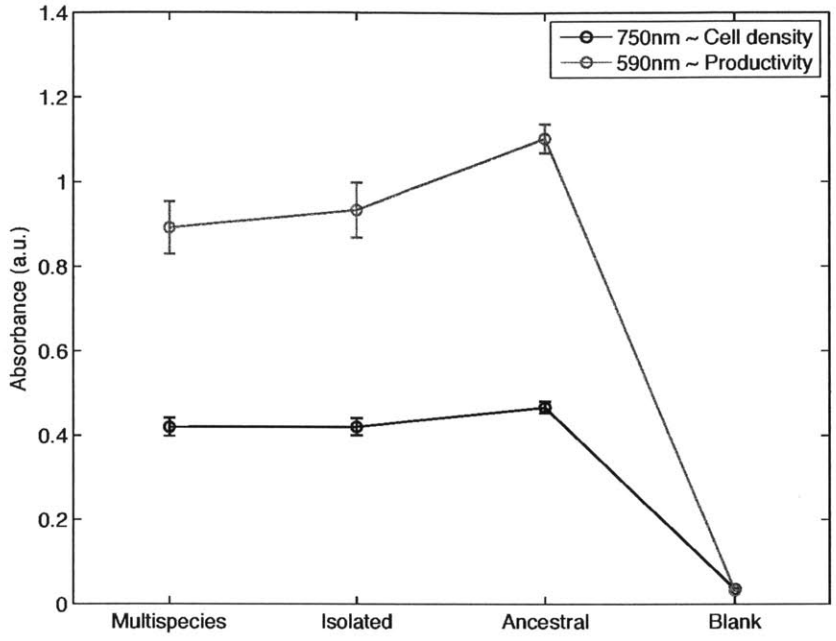

Figure S2: Optical absorbance data for different treatments. Just before the relative abundance measurements, micro plates containing the replicates for each treatment were used to measure optical absorbance of the cultures at 590nm and 750nm. At 590nm, the tetrazolium dye in the media has an absorption peak. The measurement at this wavelength gives a quantitative proxy for CO2 production (or respiration/productivity) in the cultures. At 750nm, this dye is not absorbent and the measurement at this wavelength gives a value for optical absorbance of the cultures due to cell density/biomass. The average of these measurements across all replicates for different treatments is plotted. Error bars are standard deviation. We see that there is little variation in these measurements within treatments. Moreover, multispecies and isolated treatments are similar in their mean measurements. However, at both 590 and 7590nm, ancestral treatment seems to have a larger mean and relatively less variation. The blank represents measurements over cultures inoculated with media but without cells. Cell density per optical density at 750nm were very similar across species: EA: 11.1e9 cells/mL/OD750, SM: 11.5e9

cells/mL/OD750, PF: 10.4e9 cells/mL/OD750, PA: 11.2e9 cells/mL/OD750, PV: 11.7e9 cells/mL/OD750, PP: 10.8e9 cells/mL/OD750.

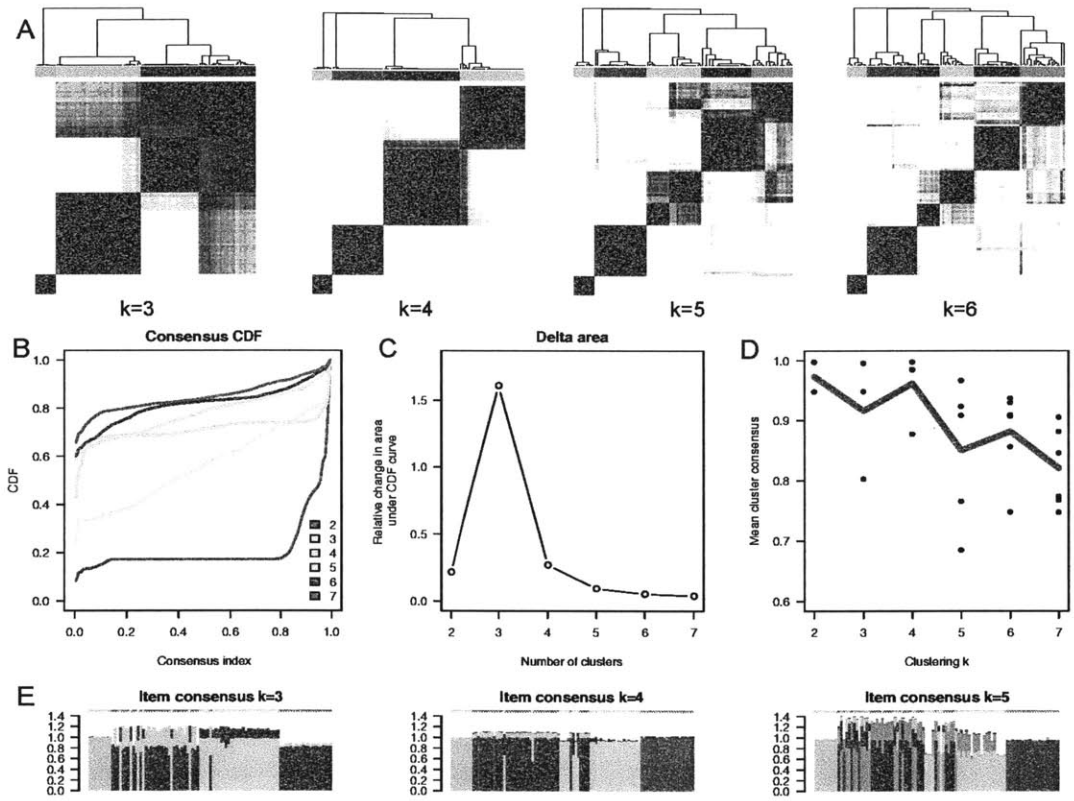

Figure S3: Consensus clustering for multispecies treatment. (A) Consensus matrix heat maps for k=3,4,5 and 6 (number of clusters). Rows and columns correspond to observations (items). Consensus values range between 0 and 1, marker by white to dark blue. Scaling is the same across all plots. A consensus value of 1 for two items means these two items clustered together 100% of the time across all subsamples, whereas a value of 0 means that two items never clustered together (see methods). A dendrogram of consensus clustering results is plotted above the columns of the heat maps, and the found clusters are color coded. **(B)** Consensus cumulative distribution function plot. This plot shows the cumulative

distribution of consensus matrix for each k (legend) estimated by a histogram of 100 bins. **(C)** Relative change in the area under the CDF curves (change between k and k-1). For k = 2, the total area under the curve is plotted. **(D)** Mean consensus value for each cluster plotted for k=2 through 7 (black dots). The red line corresponds to the average of all the cluster means for a given k. **(E)** Item consensus plots. The mean consensus of each item with all the other items in a cluster is plotted. The values for the different clusters are stacked together for each item and the stack colors correspond to the clusters indicated above the heat maps in (A). Item consensus plots for k = 3,4 and 5 is plotted. If a sample is a stable and pure member of a cluster, it would not share consensus with any clusters but just one. Stacks containing more than one large bars indicate unstable members.

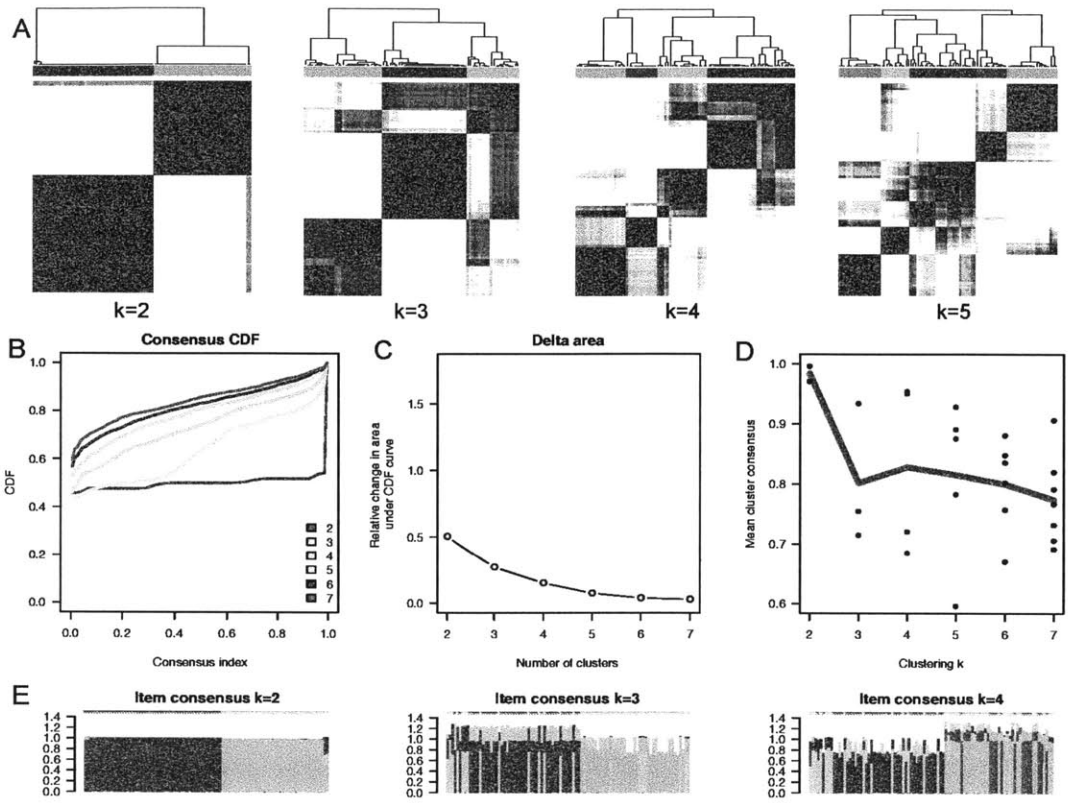

Figure S4: Consensus clustering for isolated treatment. (A) Consensus matrix heat maps for k=2,3,4 and 5 (number of clusters). Rows and columns correspond to observations (items). Consensus values range between 0 and 1, marker by white to dark blue. Scaling is the same across all plots. A consensus value of 1 for two items means these two items clustered together 100% of the time across all subsamples, whereas a value of 0 means that two items never clustered together (see methods). A dendrogram of consensus clustering results is plotted above the columns of the heat maps, and the found clusters are color coded. **(B)** Consensus cumulative distribution function plot. This plot shows the cumulative distribution of consensus matrix for each k (legend) estimated by a histogram of 100 bins. **(C)** Relative change in the area under the CDF curves (change between k and k-1). For k = 2, the total area under the curve is plotted. **(D)** Mean consensus value for each cluster plotted for k=2 through 7 (black dots). The red line corresponds to the average of all the cluster means for a given k. **(E)** Item consensus plots. The mean consensus of each

item with all the other items in a cluster is plotted. The values for the different clusters are stacked together for each item and the stack colors correspond to the clusters indicated above the heat maps in (A). Item consensus plots for k = 2,3 and 4 is plotted. If a sample is a stable and pure member of a cluster, it would not share consensus with any clusters but just one. Stacks containing more than one large bars indicate unstable members.

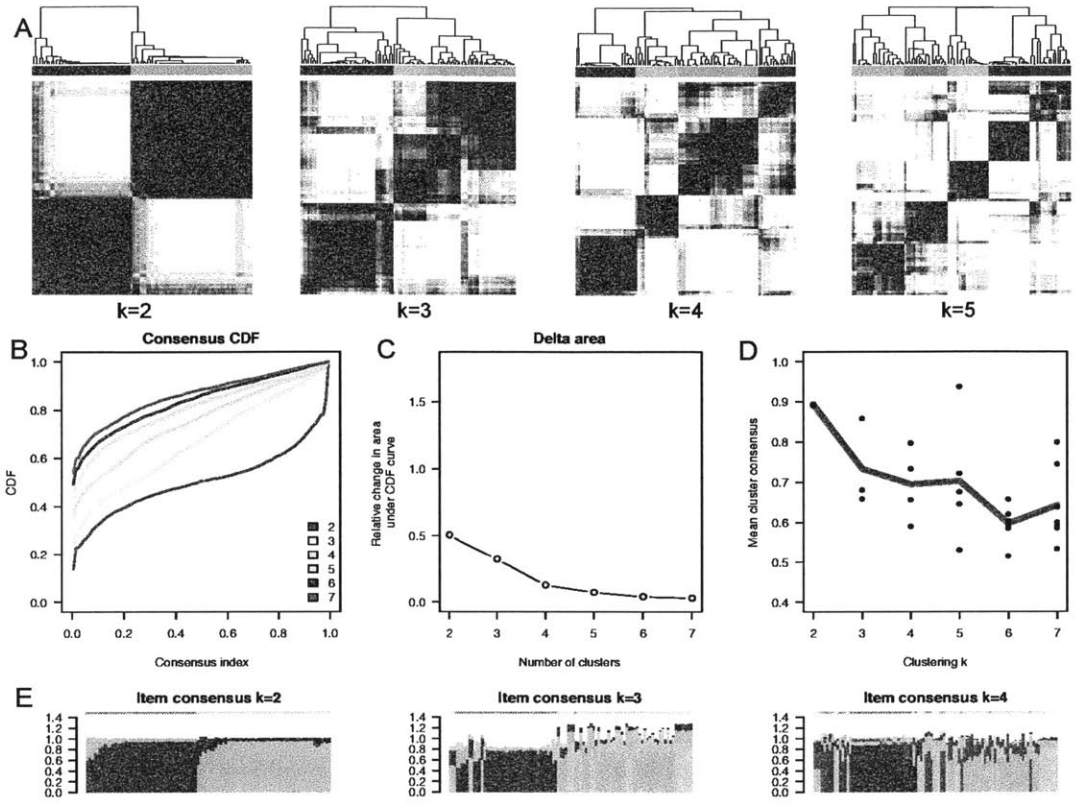

Figure S5: Consensus clustering for randomly generated data. (A) Consensus matrix heat maps for k=2,3,4 and 5 (number of clusters). Rows and columns correspond to observations (items). Consensus values range between 0 and 1, marker by white to dark blue. Scaling is the same across all plots. A consensus value of 1 for two items means these two items clustered together 100% of the time across all subsamples, whereas a value of 0 means that two items never clustered together (see methods). A dendrogram of consensus clustering results is plotted above the columns of the heat maps, and the found clusters are color coded. **(B)** Consensus cumulative distribution function plot. This plot shows the cumulative distribution of consensus matrix for each k (legend) estimated by a histogram of 100 bins. **(C)** Relative change in the area under the CDF curves (change between k and k-1). For k = 2, the total area under the curve is plotted. **(D)** Mean consensus value for each cluster plotted for k=2 through 7 (black dots). The red line corresponds to the average of all the cluster means for a given k. **(E)** Item consensus

plots. The mean consensus of each item with all the other items in a cluster is plotted. The values for the different clusters are stacked together for each item and the stack colors correspond to the clusters indicated above the heat maps in (A). Item consensus plots for k = 2,3 and 4 is plotted. If a sample is a stable and pure member of a cluster, it would not share consensus with any clusters but just one. So, stacks containing more than one large bars indicate unstable members.

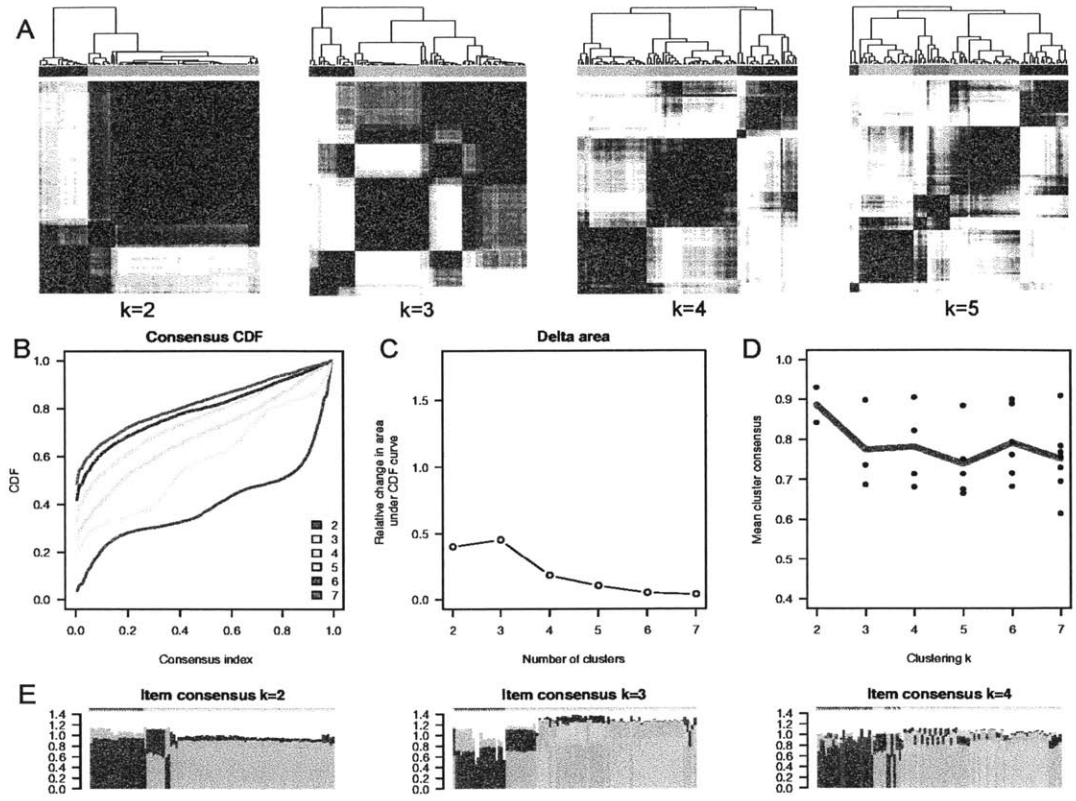

Figure S6: Consensus clustering for ancestral treatment. (A) Consensus matrix heat maps for k=2,3,4 and 5 (number of clusters). Rows and columns correspond to observations (items). Consensus values range between 0 and 1, marker by white to dark blue. Scaling is the same across all plots. A consensus value of 1 for two items means these two items clustered together 100% of the time across all subsamples, whereas a value of 0 means that two items never clustered together (see methods). A dendrogram of consensus clustering results is plotted above the columns of the heat maps, and the found clusters are color coded. **(B)** Consensus cumulative distribution function plot. This plot shows the cumulative distribution of consensus matrix for each k (legend) estimated by a histogram of 100 bins. **(C)** Relative change in the area under the CDF curves (change between k and k-1). For k = 2, the total area under the curve is plotted. **(D)** Mean consensus value for each cluster plotted for k=2 through 7 (black dots). The red line corresponds to the average of all the cluster means for a given k. **(E)** Item consensus plots. The mean consensus of each

item with all the other items in a cluster is plotted. The values for the different clusters are stacked together for each item and the stack colors correspond to the clusters indicated above the heat maps in (A). Item consensus plots for k = 2,3 and 4 is plotted. If a sample is a stable and pure member of a cluster, it would not share consensus with any clusters but just one. So, stacks containing more than one large bars indicate unstable members.

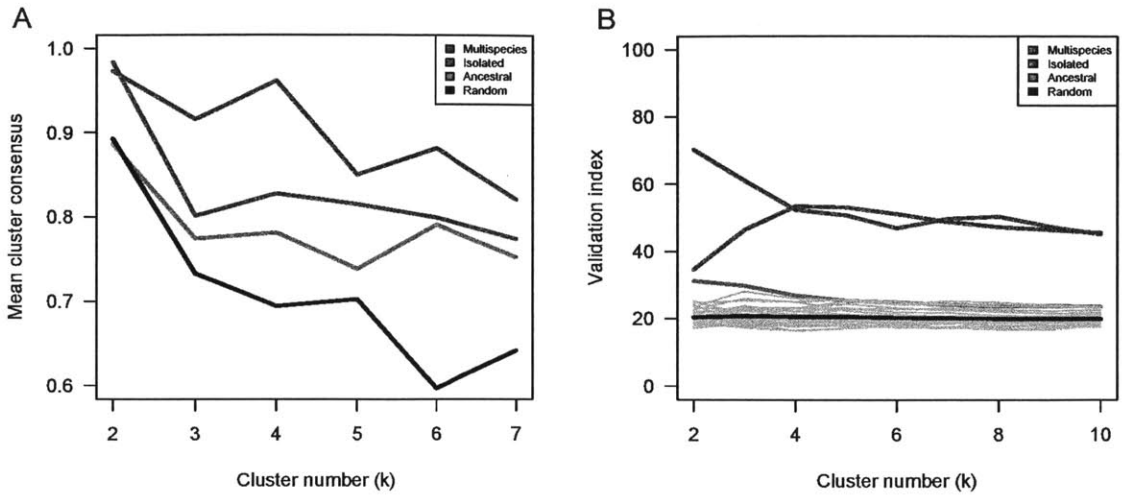

Figure S7: Comparative mean consensus plots and hierarchical clustering results for different treatments. (A) Mean consensus plots for multispecies, isolated, ancestral treatments and also for randomly generated data. **(B)** Calinski-Harabasz validation index for hierarchical clustering results for the different treatments. The optimal cluster number is at k, where the validation index is at its maximum. The higher this index value is the better the clustering. The black line represents the mean of the results for 50 randomly generated datasets (gray lines).

REFERENCES

1. Axelrod R, Hamilton WD (1981) The evolution of cooperation. Science 211: 1390–1396. Available: http://www.ncbi.nlm.nih.gov/pubmed/7466396.
2. Nowak MA (2006) Five Rules for the Evolution of Cooperation. Science 314: 1560–1563. Available: http://www.sciencemag.org/cgi/content/abstract/314/5805/1560.
3. Frank SA (1998) Foundations of Social Evolution. Economic Analysis 82: 343–344. Available: http://books.google.com/books?id=i84aDNaxyOEC.
4. Nowak MA, Tarnita CE, Wilson EO (2010) The evolution of eusociality. Nature 466: 1057–1062. Available: http://www.nature.com/doifinder/10.1038/nature09205.
5. West S (2007) Social Evolution Theory in Microbes: Cooperation and Conflict. Annual Review of Ecology Evolution and Systematics 38. Available: http://arjournals.annualreviews.org/doi/abs/10.1146/annurev.ecolsys.38.091206.095740.
6. West SA, Diggle SP, Buckling A, Gardner A, Griffin AS (2007) The Social Lives of Microbes. Annual Review of Ecology Evolution and Systematics 38: 53–77. Available: http://arjournals.annualreviews.org/doi/abs/10.1146/annurev.ecolsys.38.091206.095740.
7. Smukalla S, Caldara M, Pochet N, Beauvais A, Yan C, et al. (2009) FLO1 is a variable green beard gene that drives biofilm-like cooperation in budding yeast. Cell 135: 726–737. doi:10.1016/j.cell.2008.09.037.FLO1.
8. Queller DC, Ponte E, Bozzaro S, Strassmann JE (2003) Single-gene greenbeard effects in the social amoeba Dictyostelium discoideum. Science 299: 105–106. Available: http://www.ncbi.nlm.nih.gov/pubmed/12511650.
9. Rainey PB, Rainey K (2003) Evolution of cooperation and conflict in experimental bacterial populations. Nature 425: 72–74. Available: http://www.ncbi.nlm.nih.gov/pubmed/12955142.
10. MacLean RC, Gudelj I (2006) Resource competition and social conflict in experimental populations of yeast. Nature 441: 498–501. Available: http://opus.bath.ac.uk/7039/.
11. Diggle SP, Griffin AS, Campbell GS, West SA (2007) Cooperation and conflict in quorum-sensing bacterial populations. Nature 450: 411–414. Available: http://www.ncbi.nlm.nih.gov/pubmed/18004383.
12. Chuang JS, Rivoire O, Leibler S (2009) Simpson's paradox in a synthetic microbial system. Science 323: 272–275. Available: http://www.ncbi.nlm.nih.gov/pubmed/19131632.
13. Brockhurst MA, Buckling A, Gardner A (2007) Cooperation peaks at intermediate disturbance. Current Biology 17: 761–765. doi:10.1016/j.cub.2007.02.057.
14. Brockhurst MA, Habets MGJL, Libberton B, Buckling A, Gardner A (2010) Ecological drivers of the evolution of public-goods cooperation in bacteria.

Ecology 91: 334–340. Available: http://www.ncbi.nlm.nih.gov/pubmed/20391997.
15. Little AEF, Robinson CJ, Peterson SB, Raffa KF, Handelsman J (2008) Rules of engagement: interspecies interactions that regulate microbial communities. Annual Review of Microbiology 62: 375–401. Available: http://www.ncbi.nlm.nih.gov/pubmed/18544040.
16. Thompson JN (1999) The Evolution of Species Interactions. Science 284: 2116–2118. Available: http://www.ncbi.nlm.nih.gov/pubmed/10381869.
17. Connell JH (1961) The influence of interspecific competition and other factors on the distribution of the barnacle Chthamalus stellatus. Ecology 42: 710–723. Available: http://www.esajournals.org/doi/abs/10.2307/1933500.
18. Schoener TW (1983) Field experiments on interspecific competition. The American Naturalist 122: 240–285. Available: http://www.jstor.org/stable/2461233.
19. Schluter D (1994) Experimental evidence that competition promotes divergence in adaptive radiation. Science 266: 798–801. Available: http://www.ncbi.nlm.nih.gov/pubmed/17730400.
20. Grant PR, Grant BR (2006) Evolution of character displacement in Darwin's finches. Science 313: 224–226. Available: http://www.ncbi.nlm.nih.gov/pubmed/16840700.
21. Korb J, Foster KR (2010) Ecological competition favours cooperation in termite societies. Ecology letters 13: 754–760. Available: http://www.ncbi.nlm.nih.gov/pubmed/20584170. Accessed 5 July 2011.
22. Harrison F, Paul J, Massey RC, Buckling A (2008) Interspecific competition and siderophore-mediated cooperation in Pseudomonas aeruginosa. The ISME journal 2: 49–55. Available: http://dx.doi.org/10.1038/ismej.2007.96.
23. Hibbing ME, Fuqua C, Parsek MR, Peterson SB (2010) Bacterial competition: surviving and thriving in the microbial jungle. Nature Reviews Microbiology 8: 15–25. Available: http://www.ncbi.nlm.nih.gov/pubmed/19946288.
24. Mitri S, Xavier JB, Foster KR (2011) Social evolution in multispecies biofilms. Proceedings of the National Academy of Sciences 108: 10839–10846.
25. Greig D, Travisano M (2004) The Prisoner's Dilemma and polymorphism in yeast SUC genes. Proceedings of the Royal Society of London Series B Biological Sciences 271: S25. Available: http://rspb.royalsocietypublishing.org/content/271/Suppl_3/S25.short.
26. Gore J, Youk H, Oudenaarden AV (2009) Snowdrift game dynamics and facultative cheating in yeast. Nature 459: 253–256. Available: http://www.ncbi.nlm.nih.gov/pubmed/19349960.
27. Reid SJ, Abratt VR (2005) Sucrose utilisation in bacteria: genetic organisation and regulation. Applied Microbiology and Biotechnology 67: 312–321. Available: http://www.ncbi.nlm.nih.gov/pubmed/15660210.
28. Henderson PJ, Giddens RA, Jones-Mortimer MC (1977) Transport of galactose, glucose and their molecular analogues by Escherichia coli K12. The Biochemical journal 162: 309–320. Available: http://www.pubmedcentral.nih.gov/articlerender.fcgi?artid=1164603.

29. Davison BH, Stephanopoulos G (1986) Effect of pH oscillations on a competing mixed culture. Biotechnology and Bioengineering 28: 1127–1137.
30. Foster JW (2004) Escherichia coli acid resistance: tales of an amateur acidophile. Nature Reviews Microbiology 2: 898–907. Available: http://www.ncbi.nlm.nih.gov/pubmed/15494746.
31. Okafor N (1975) Microbiology of Nigerian Palm Wine with Particular Reference to Bacteria. Journal of Applied Microbiology 38: 81–88. Available: http://doi.wiley.com/10.1111/j.1365-2672.1975.tb00507.x. Accessed 26 October 2011.
32. Kuramae EE, Gamper HA, Yergeau E, Piceno YM, Brodie EL, et al. (2010) Microbial secondary succession in a chronosequence of chalk grasslands. The ISME journal 4: 711–715. Available: http://www.ncbi.nlm.nih.gov/pubmed/20164861.
33. Koenig JE, Spor A, Scalfone N, Fricker AD, Stombaugh J, et al. (2011) Succession of microbial consortia in the developing infant gut microbiome. Proceedings of the National Academy of Sciences 108 : 4578–4585.
34. Murdoch WW (1991) The shift from an equilibrium to a non-equilibrium paradigm in ecology. Bulletin of the Ecological Society of America 72: 49–51.
35. Tilman D (1982) Resource competition and community structure. Princeton University Press.
36. Thomson JM, Gaucher EA, Burgan MF, De Kee DW, Li T, et al. (2005) Resurrecting ancestral alcohol dehydrogenases from yeast. Nature Genetics 37: 630–635. Available: http://www.ncbi.nlm.nih.gov/pubmed/15864308.
37. Molles MC (2010) Ecology: Concepts and Applications. McGraw-Hill .
38. Sexton JP, McIntyre PJ, Angert AL, Rice KJ (2009) Evolution and Ecology of Species Range Limits. Annual Review of Ecology Evolution and Systematics 40: 415–436. Available: http://arjournals.annualreviews.org/doi/abs/10.1146/annurev.ecolsys.110308.120317.
39. Ross-Gillespie A, Gardner A, Buckling A, West SA, Griffin AS (2009) Density dependence and cooperation: theory and a test with bacteria. Evolution: International Journal of Organic Evolution 63: 2315–2325. Available: http://www.ncbi.nlm.nih.gov/pubmed/19453724.
40. Lesuisse E, Blaiseau PL, Dancis A, Camadro JM (2001) Siderophore uptake and use by the yeast Saccharomyces cerevisiae. Microbiology 147: 289–298. Available: http://www.ncbi.nlm.nih.gov/pubmed/11158346.
41. Chen J, Weimer P (2001) Competition among three predominant ruminal cellulolytic bacteria in the absence or presence of non-cellulolytic bacteria. Microbiology 147: 21–30. Available: http://www.ncbi.nlm.nih.gov/pubmed/11160797.
42. Flint HJ, Bayer EA, Rincon MT, Lamed R, White BA (2008) Polysaccharide utilization by gut bacteria: potential for new insights from genomic analysis. Nature Reviews Microbiology 6: 121–131. Available: http://www.ncbi.nlm.nih.gov/pubmed/18180751.

43. Flint HJ, Duncan SH, Scott KP, Louis P (2007) Interactions and competition within the microbial community of the human colon: links between diet and health. Environmental Microbiology 9: 1101–1111. Available: http://www.ncbi.nlm.nih.gov/pubmed/17472627.
44. Belenguer A, Duncan SH, Calder AG, Holtrop G, Louis P, et al. (2006) Two Routes of Metabolic Cross-Feeding between Bifidobacterium adolescentis and Butyrate-Producing Anaerobes from the Human Gut. Society 72: 3593–3599. doi:10.1128/AEM.72.5.3593.
45. Loeb SC, Hooper RG (1997) An experimental test of interspecific competition for red-cockaded woodpecker cavities. The Journal of Wildlife Management 61: 1268–1280. Available: http://www.jstor.org/stable/3802126?origin=crossref.
46. Caro TM, Stoner CJ (2003) The potential for interspecific competition among African carnivores. Biological Conservation 110: 67–75. Available: http://linkinghub.elsevier.com/retrieve/pii/S0006320702001775.
47. Youk H, Van Oudenaarden A (2009) Growth landscape formed by perception and import of glucose in yeast. Nature 462: 875–879. Available: http://www.nature.com/nature/journal/vaop/ncurrent/abs/nature08653.html.
48. Gancedo JM (1998) Yeast Carbon Catabolite Repression. Microbiology and Molecular Biology Reviews 62: 334–361. Available: http://www.pubmedcentral.nih.gov/articlerender.fcgi?artid=98918&tool=pmcentrez&rendertype=abstract.
49. Ozcan S, Vallier LG, Flick JS, Carlson M, Johnston M (1997) Expression of the SUC2 gene of Saccharomyces cerevisiae is induced by low levels of glucose. Yeast 13: 127–137. Available: http://www.ncbi.nlm.nih.gov/pubmed/9046094.
50. Johnson MTJ, Stinchcombe JR (2007) An emerging synthesis between community ecology and evolutionary biology. Trends in Ecology & Evolution 22: 250–257. Available: http://www.ncbi.nlm.nih.gov/pubmed/17296244.
51. Turcotte MM, Corrin MSC, Johnson MTJ (2012) Adaptive Evolution in Ecological Communities. PLoS Biology 10: e1001332. Available: http://dx.plos.org/10.1371/journal.pbio.1001332.
52. Lavergne S, Mouquet N, Thuiller W, Ronce O (2010) Biodiversity and Climate Change: Integrating Evolutionary and Ecological Responses of Species and Communities. Annual Review of Ecology Evolution and Systematics 41: 321–350. Available: http://www.annualreviews.org/doi/abs/10.1146/annurev-ecolsys-102209-144628.
53. De Mazancourt C, Johnson E, Barraclough TG (2008) Biodiversity inhibits species' evolutionary responses to changing environments. Ecology Letters 11: 380–388. Available: http://www.ncbi.nlm.nih.gov/pubmed/18248449.
54. Strauss SY, Sahli H, Conner JK (2005) Toward a more trait-centered approach to diffuse (co)evolution. New Phytologist 165: 81–89. Available: http://www.ncbi.nlm.nih.gov/pubmed/15720623.

55. Lawrence D, Fiegna F, Behrends V, Bundy JG, Phillimore AB, et al. (2012) Species Interactions Alter Evolutionary Responses to a Novel Environment. PLoS Biology 10: e1001330. Available: http://dx.plos.org/10.1371/journal.pbio.1001330.
56. Stinchcombe JR, Rausher MD (2001) Diffuse selection on resistance to deer herbivory in the ivyleaf morning glory, Ipomoea hederacea. The American naturalist 158: 376–388. Available: http://www.ncbi.nlm.nih.gov/pubmed/18707334.
57. Burbrink FT, Chen X, Myers EA, Brandley MC, Pyron RA (2012) Evidence for determinism in species diversification and contingency in phenotypic evolution during adaptive radiation. Proceedings of the Royal Society B Biological Sciences. Available: http://rspb.royalsocietypublishing.org/content/early/2012/09/26/rspb.2012.1669.abstract.
58. Herron MD, Doebeli M (2013) Parallel evolutionary dynamics of adaptive diversification in Escherichia coli. PLoS Biology 11: e1001490.
59. Gravel D, Bell T, Barbera C, Bouvier T, Pommier T, et al. (2011) Experimental niche evolution alters the strength of the diversity–productivity relationship. Nature 469: 89–92. Available: http://www.ncbi.nlm.nih.gov/pubmed/21131946.
60. Foster KR, Bell T (2012) Competition, not Cooperation, Dominates Interactions among Culturable Microbial Species. Current biology CB: 1–6. doi:10.1016/j.cub.2012.08.005.
61. Monti S, Tamayo P, Mesirov J, Golub T (2003) Consensus Clustering: A Resampling-Based Method for Class Discovery and Visualization of Gene Expression Microarray Data. Machine Learning 52: 91–118. Available: http://www.springerlink.com/index/V2LN11K7071V1H7V.pdf.
62. Stern DL, Orgogozo V (2009) Is genetic evolution predictable? Science 323: 746–751. Available: http://www.ncbi.nlm.nih.gov/pubmed/19197055.
63. Losos JB, Jackman TR, Larson A, De Queiroz K, Rodriguez-Schettino L (1998) Contingency and determinism in replicated adaptive radiations of island lizards. Science 279: 2115–2118. Available: http://www.sciencemag.org/cgi/doi/10.1126/science.279.5359.2115.
64. Buckley TR, Attanayake D, Bradler S (2009) Extreme convergence in stick insect evolution: phylogenetic placement of the Lord Howe Island tree lobster. Proceedings of the Royal Society B Biological Sciences 276: 1055–1062. Available: http://www.pubmedcentral.nih.gov/articlerender.fcgi?artid=2679072&tool=pmcentrez&rendertype=abstract.
65. Poe S, Goheen JR, Hulebak EP (2007) Convergent exaptation and adaptation in solitary island lizards. Proceedings of the Royal Society B Biological Sciences 274: 2231–2237. Available: http://www.pubmedcentral.nih.gov/articlerender.fcgi?artid=2287374&tool=pmcentrez&rendertype=abstract.

66. Reding DM, Foster JT, James HF, Pratt HD, Fleischer RC (2009) Convergent evolution of "creepers" in the Hawaiian honeycreeper radiation. Biology Letters 5: 221–224. Available: http://www.pubmedcentral.nih.gov/articlerender.fcgi?artid=2665804&tool=pmcentrez&rendertype=abstract.
67. Duponchelle F, Paradis E, Ribbink AJ, Turner GF (2008) Parallel life history evolution in mouthbrooding cichlids from the African Great Lakes. Proceedings of the National Academy of Sciences of the United States of America 105: 15475–15480. Available: http://dx.doi.org/10.1073/pnas.0802343105.
68. Cooper TF, Remold SK, Lenski RE, Schneider D (2008) Expression Profiles Reveal Parallel Evolution of Epistatic Interactions Involving the CRP Regulon in Escherichia coli. PLoS Genetics 4: 10. Available: http://www.pubmedcentral.nih.gov/articlerender.fcgi?artid=2242816&tool=pmcentrez&rendertype=abstract.
69. Bollback JP, Huelsenbeck JP (2009) Parallel Genetic Evolution Within and Between Bacteriophage Species of Varying Degrees of Divergence. Genetics 181: 225–234. Available: http://www.pubmedcentral.nih.gov/articlerender.fcgi?artid=2621170&tool=pmcentrez&rendertype=abstract.
70. Meyer JR, Dobias DT, Weitz JS, Barrick JE, Quick RT, et al. (2012) Repeatability and Contingency in the Evolution of a Key Innovation in Phage Lambda. Science 335: 428–432. Available: http://www.sciencemag.org/cgi/doi/10.1126/science.1214449.
71. Wichman HA, Badgett MR, Scott LA, Boulianne CM, Bull JJ (1999) Different Trajectories of Parallel Evolution During Viral Adaptation. Science 285: 422–424. Available: http://www.sciencemag.org/cgi/doi/10.1126/science.285.5426.422.
72. Shindo C, Aranzana MJ, Lister C, Baxter C, Nicholls C, et al. (2005) Role of FRIGIDA and FLOWERING LOCUS C in determining variation in flowering time of Arabidopsis. Plant Physiology 138: 1163–1173. Available: http://www.plantphysiol.org/content/138/2/1163.short.
73. ffrench-Constant RH, Pittendrigh B, Vaughan A, Anthony N (1998) Why are there so few resistance-associated mutations in insecticide target genes? Philosophical Transactions of the Royal Society of London - Series B: Biological Sciences 353: 1685–1693. Available: http://www.pubmedcentral.nih.gov/articlerender.fcgi?artid=1692388&tool=pmcentrez&rendertype=abstract.
74. Stern DL, Orgogozo V (2008) The Loci of Evolution: How Predictable is Genetic Evolution? Evolution: International Journal of Organic Evolution 62: 2155–2177. Available: http://www.pubmedcentral.nih.gov/articlerender.fcgi?artid=2613234&tool=pmcentrez&rendertype=abstract.
75. Kiontke K, Barrière A, Kolotuev I, Podbilewicz B, Sommer R, et al. (2007) Trends, stasis, and drift in the evolution of nematode vulva development.

Current Biology 17: 1925–1937. Available: http://www.ncbi.nlm.nih.gov/pubmed/18024125.

76. Wilkerson MD, Hayes DN (2010) ConsensusClusterPlus: a class discovery tool with confidence assessments and item tracking. Bioinformatics 26: 1572–1573. Available: http://www.pubmedcentral.nih.gov/articlerender.fcgi?artid=2881355&tool=pmcentrez&rendertype=abstract.